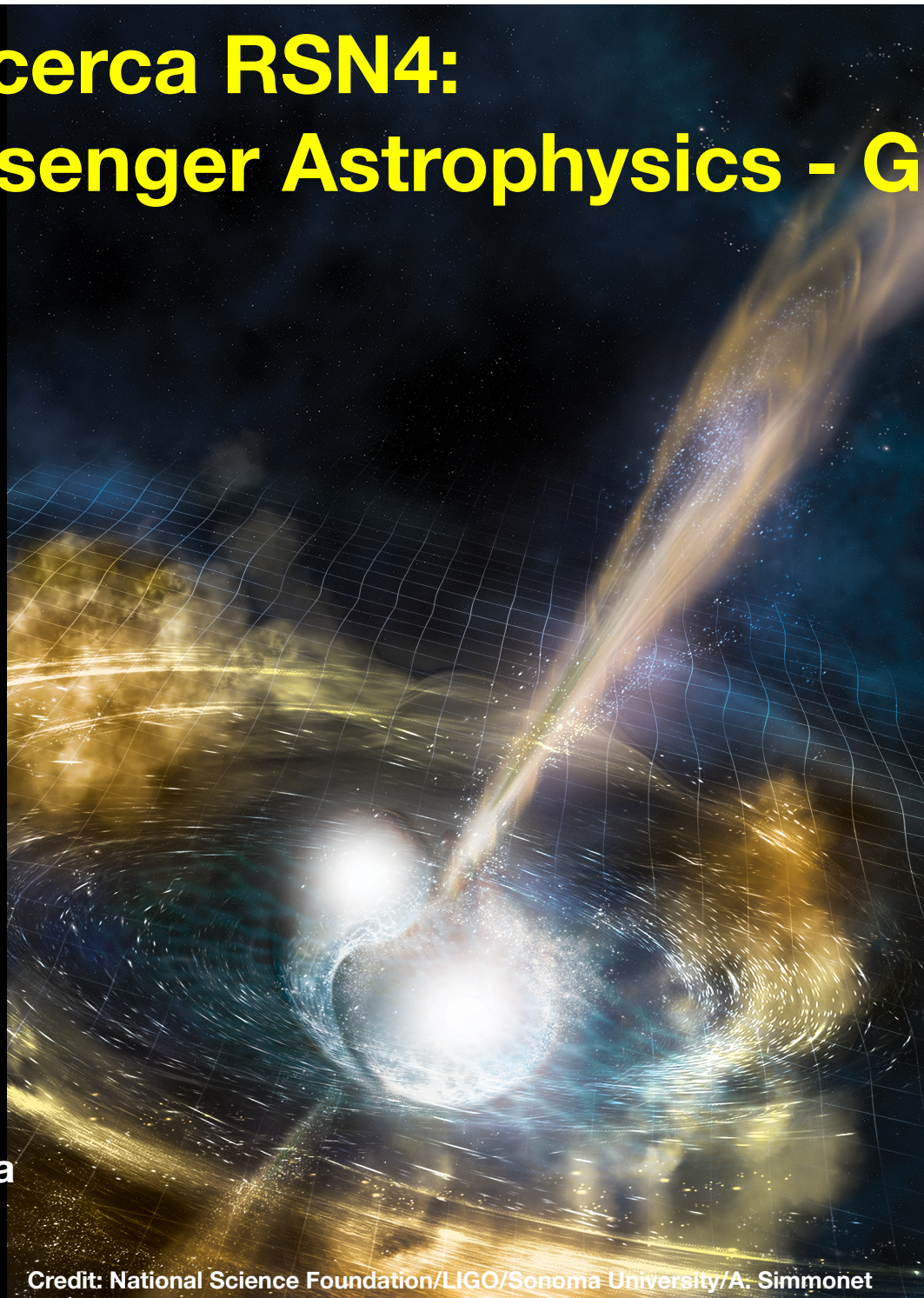


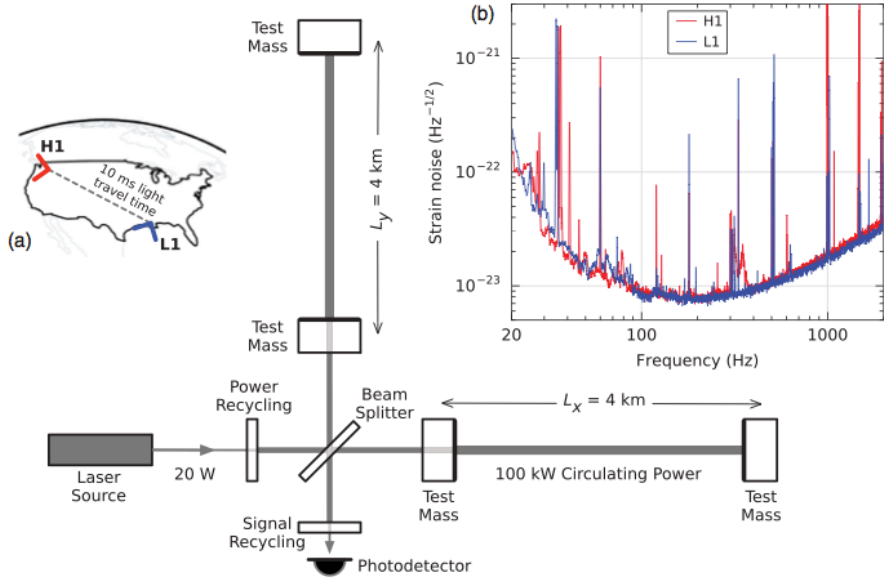
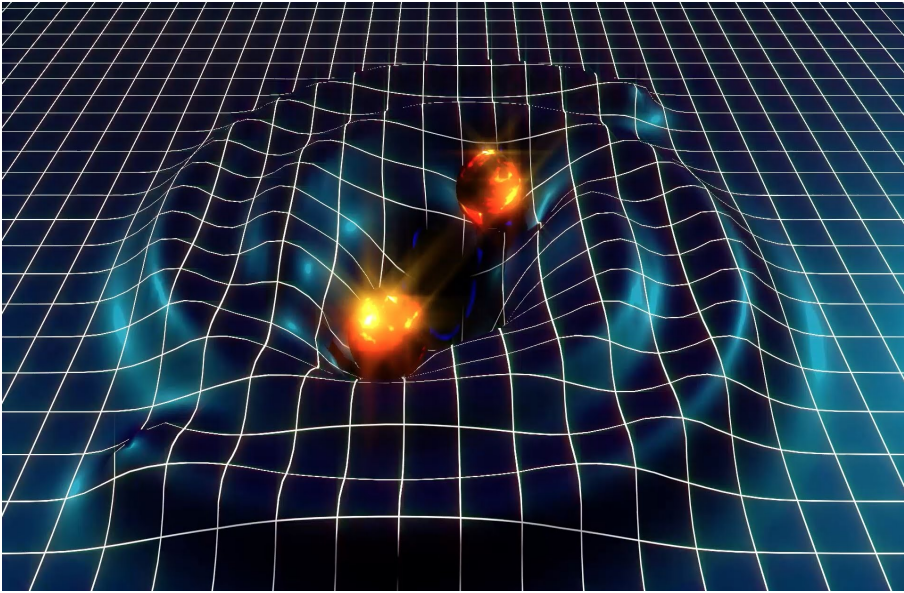
Linee di ricerca RSN4: Multi-Messenger Astrophysics - GW

Paolo D'Avanzo
INAF – Osservatorio
Astronomico di Brera

Credit: National Science Foundation/LIGO/Sonoma University/A. Simmonet



The GW era



The GW era: GW 150914



Selected for a **Viewpoint** in *Physics*
PHYSICAL REVIEW LETTERS week ending
 PRL 116, 061102 (2016) 12 FEBRUARY 2016



Observation of Gravitational Waves from a Binary Black Hole Merger

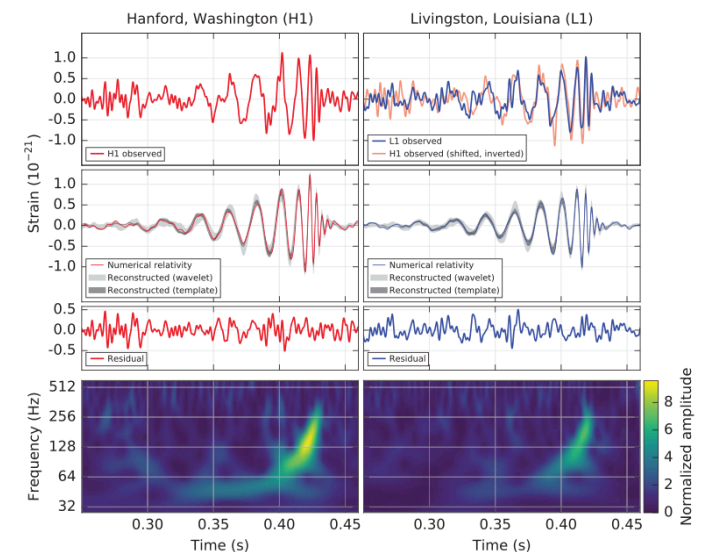
B. P. Abbott *et al.**

(LIGO Scientific Collaboration and Virgo Collaboration)

(Received 21 January 2016; published 11 February 2016)

On September 14, 2015 at 09:50:45 UTC the two detectors of the Laser Interferometer Gravitational-Wave Observatory simultaneously observed a transient gravitational-wave signal. The signal sweeps upwards in frequency from 35 to 250 Hz with a peak gravitational-wave strain of 1.0×10^{-21} . It matches the waveform predicted by general relativity for the inspiral and merger of a pair of black holes and the ringdown of the resulting single black hole. The signal was observed with a matched-filter signal-to-noise ratio of 24 and a false alarm rate estimated to be less than 1 event per 203 000 years, equivalent to a significance greater than 5.1σ . The source lies at a luminosity distance of 410^{+160}_{-180} Mpc corresponding to a redshift $z = 0.09^{+0.03}_{-0.04}$. In the source frame, the initial black hole masses are $36^{+5}_{-4} M_{\odot}$ and $29^{+4}_{-4} M_{\odot}$, and the final black hole mass is $62^{+4}_{-4} M_{\odot}$, with $3.0^{+0.5}_{-0.5} M_{\odot} c^2$ radiated in gravitational waves. All uncertainties define 90% credible intervals. These observations demonstrate the existence of binary stellar-mass black hole systems. This is the first direct detection of gravitational waves and the first observation of a binary black hole merger.

DOI: 10.1103/PhysRevLett.116.061102



Primary black hole mass	$36^{+5}_{-4} M_{\odot}$
Secondary black hole mass	$29^{+4}_{-4} M_{\odot}$
Final black hole mass	$62^{+4}_{-4} M_{\odot}$
Final black hole spin	$0.67^{+0.05}_{-0.07}$
Luminosity distance	410^{+160}_{-180} Mpc
Source redshift z	$0.09^{+0.03}_{-0.04}$

GW 150914 – EM search



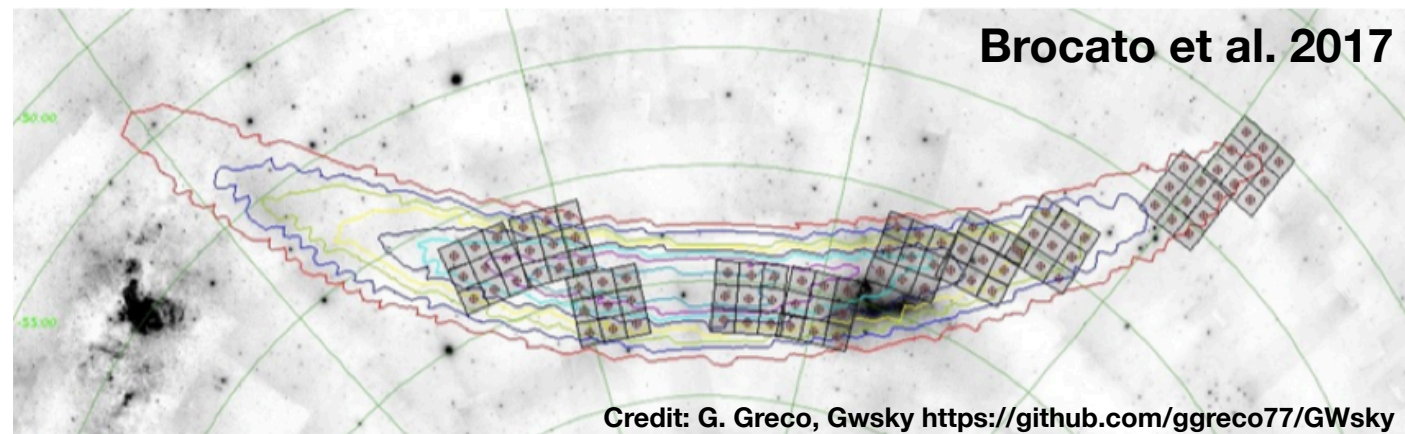
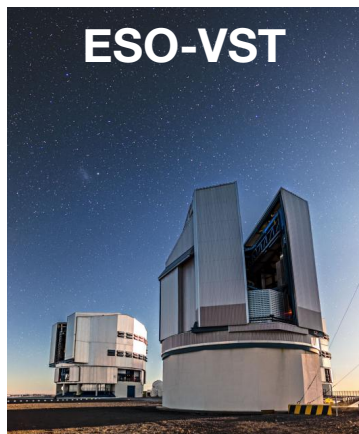
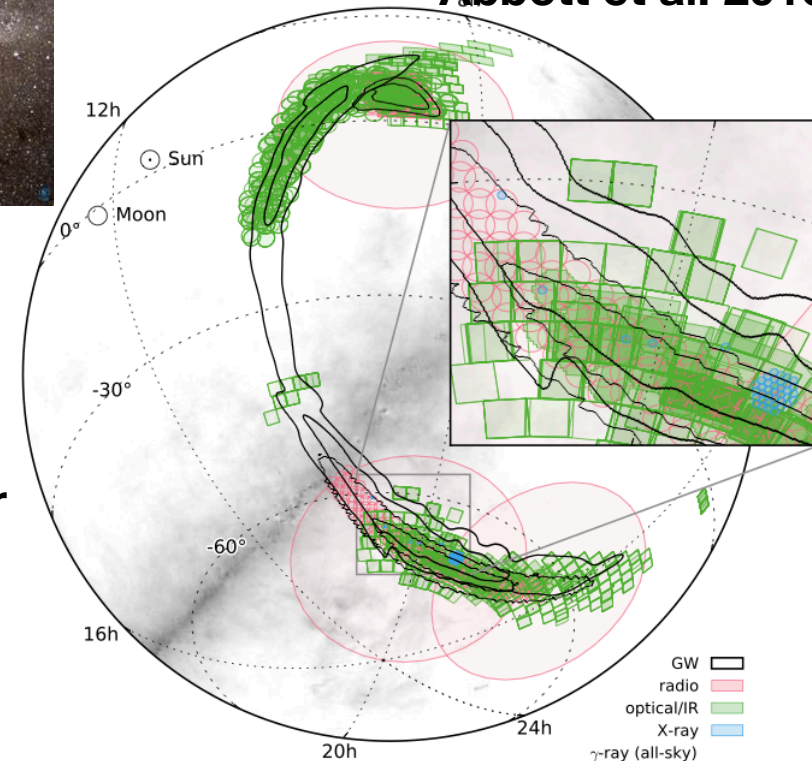
600 deg² skymap from LIGO/Virgo
Huge observational effort, mainly with wide-field facilities

No EM counterpart found

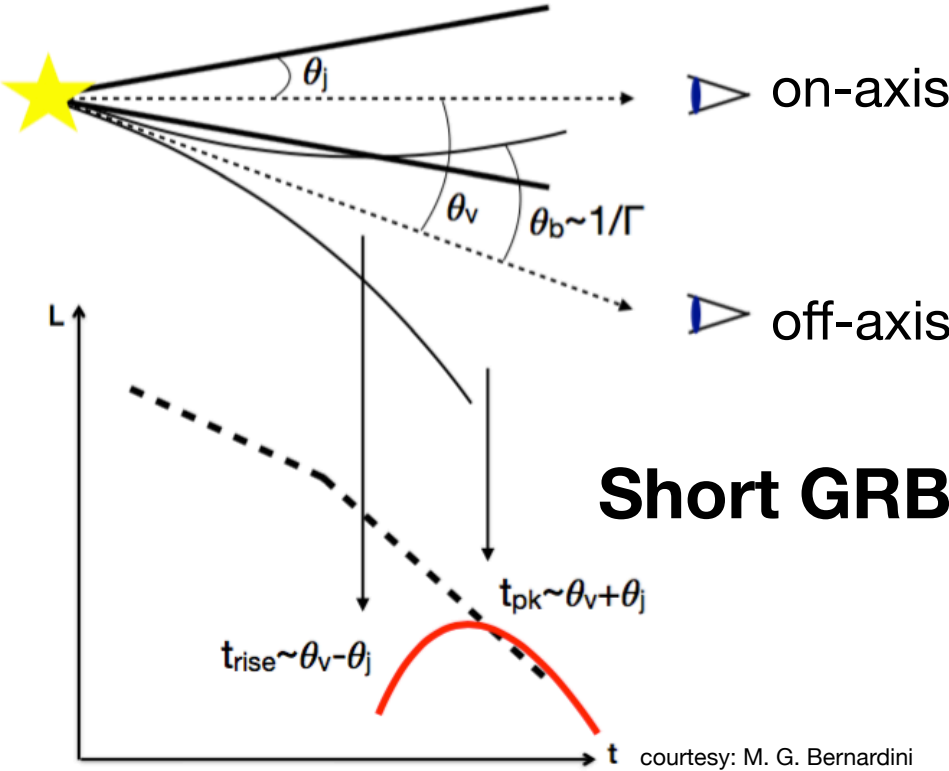
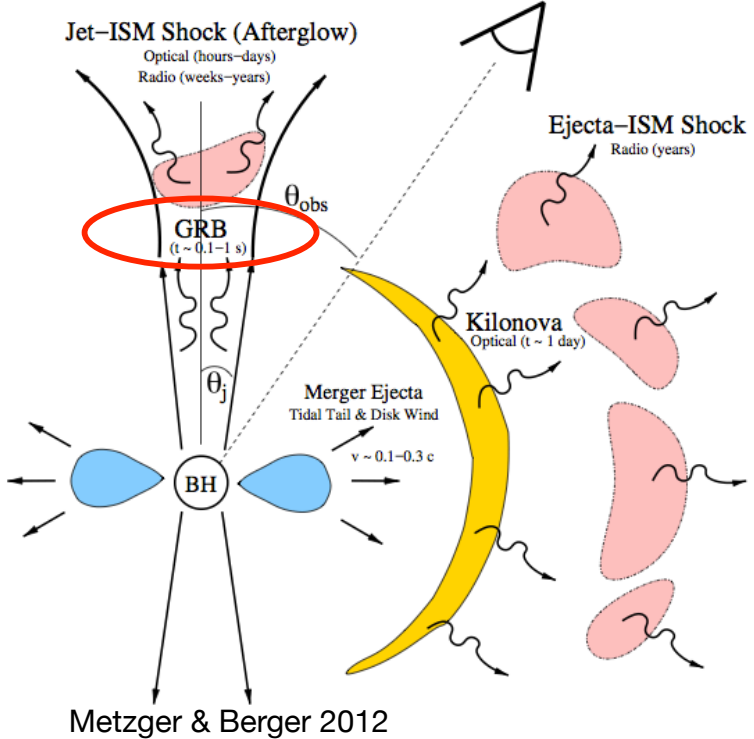
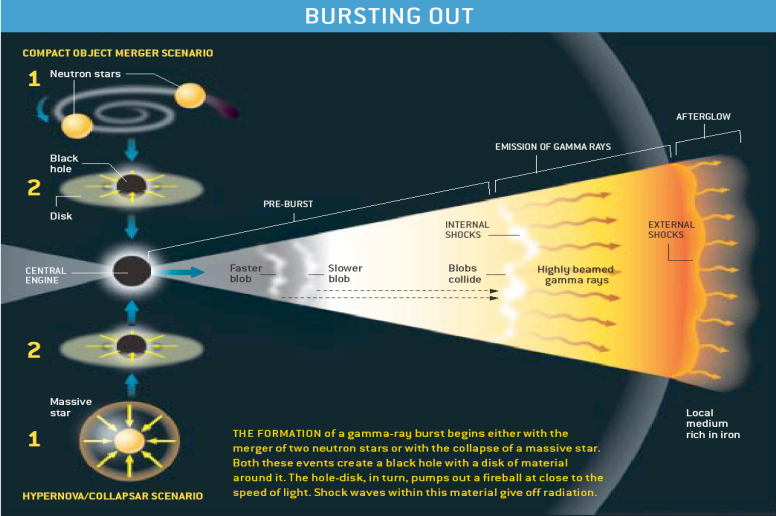
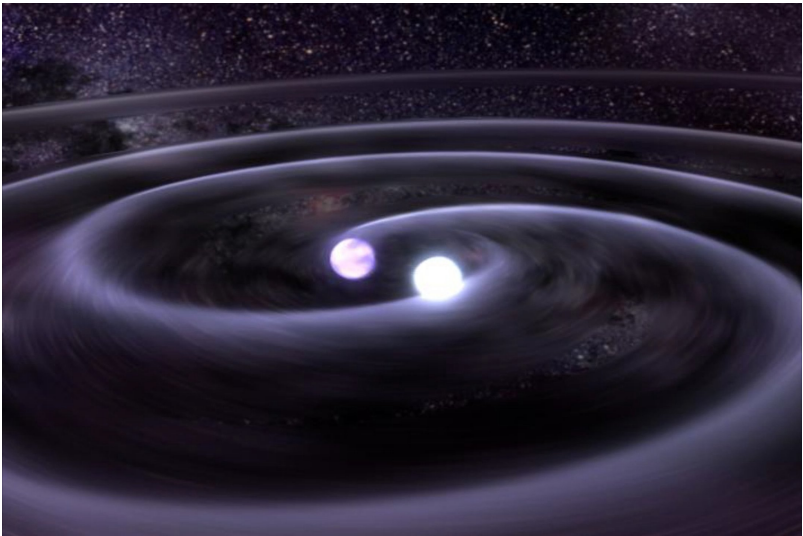
No EM counterpart expected from BHBH merger
Expected EM counterparts for NSNS/NSBH merger:

- Short GRBs (beamed emission)
- Kilonovae (isotropic emission)

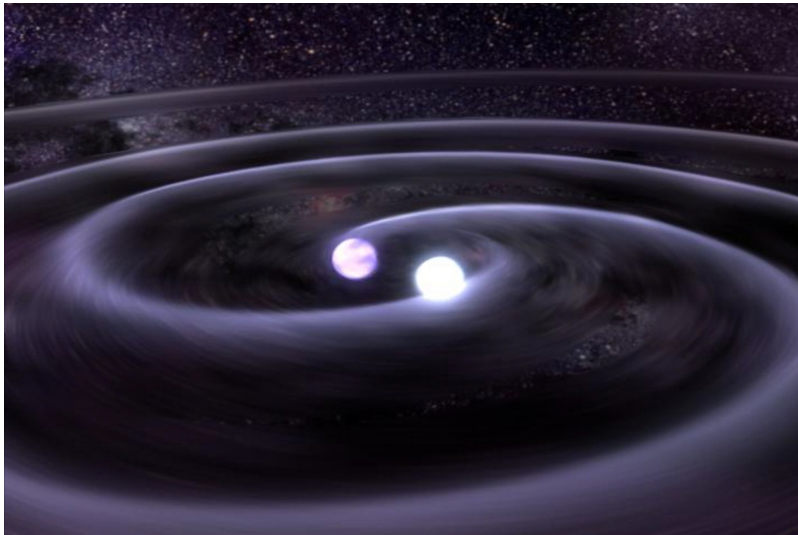
Abbott et al. 2016



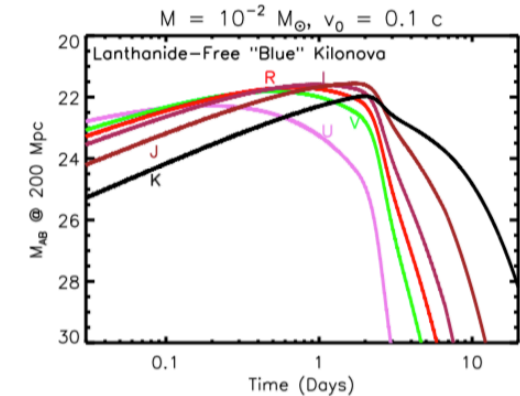
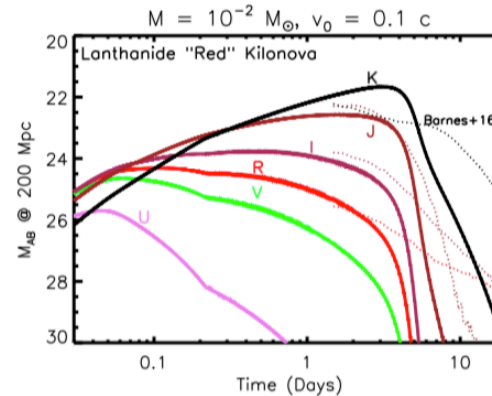
NS-NS / NS-BH electromagnetic counterparts



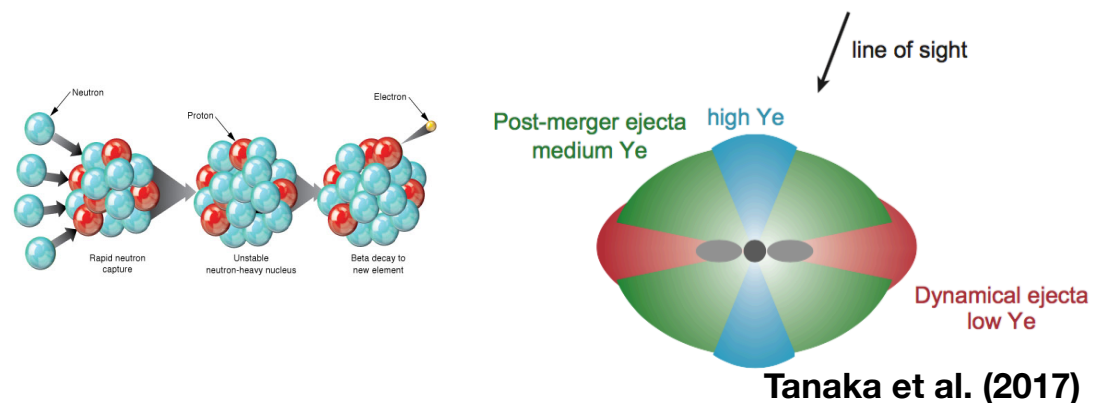
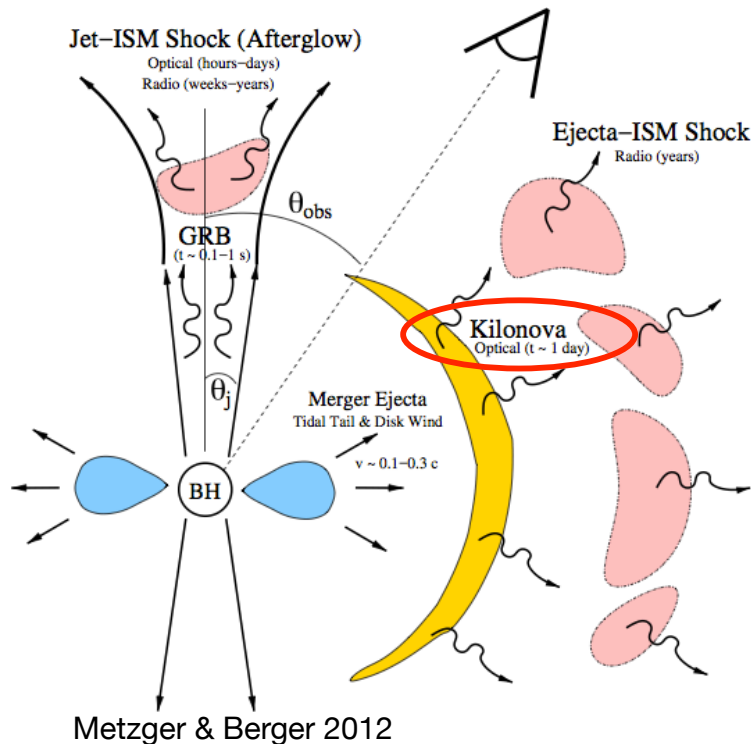
NS-NS / NS-BH electromagnetic counterparts



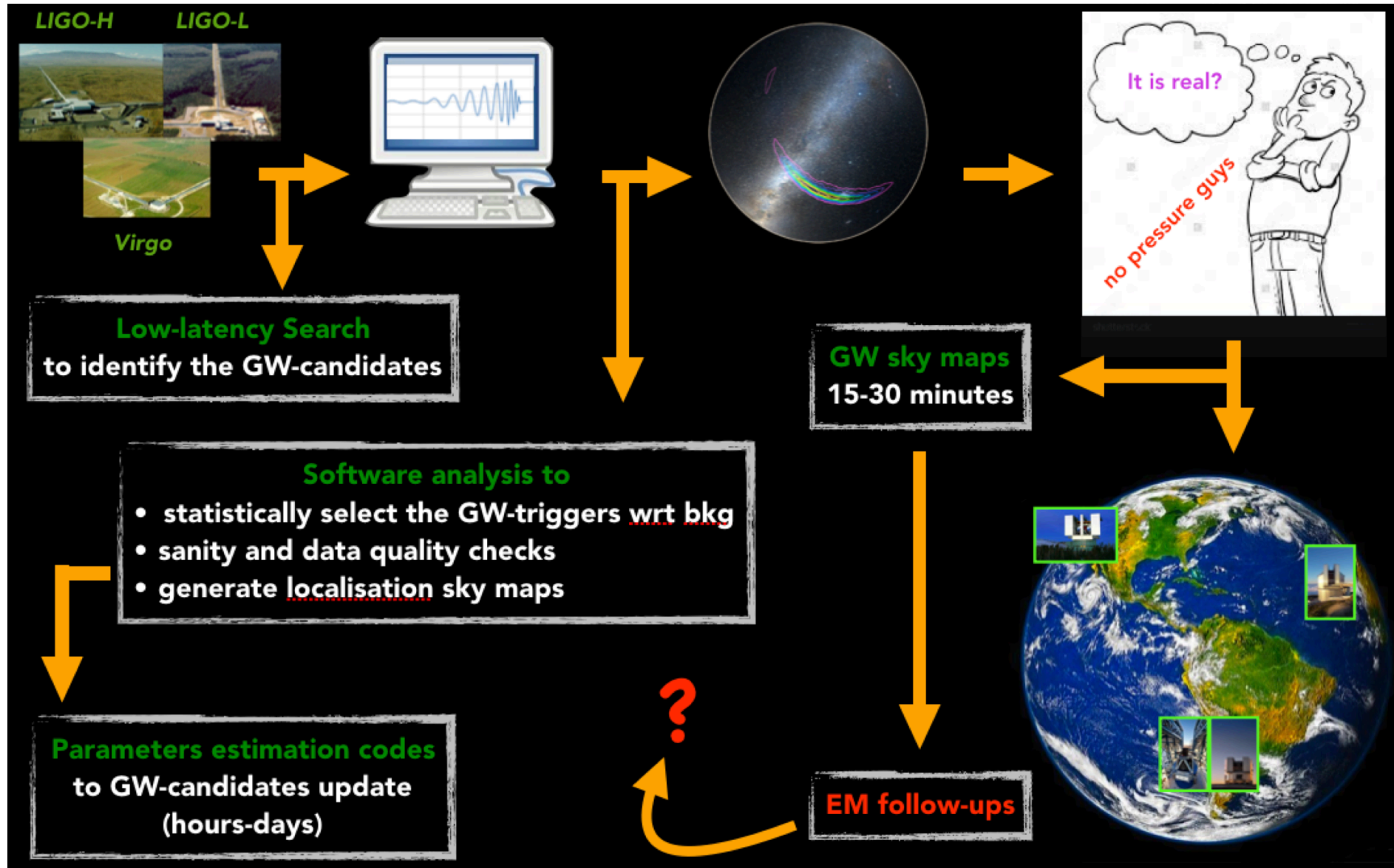
Kilonova



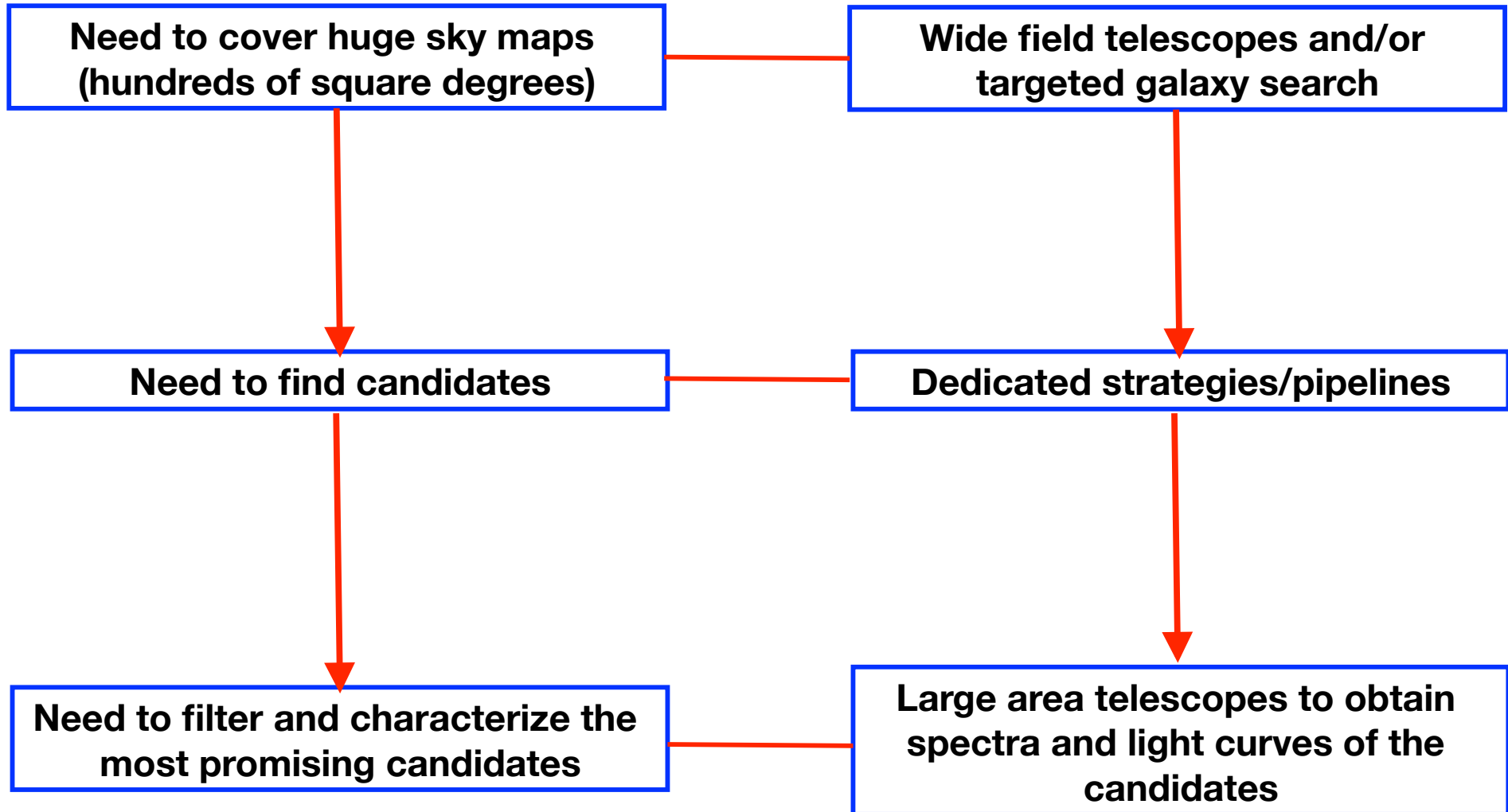
A key signature of an NS-NS/NS-BH binary merger is the production of a so-called “kilonova” (aka “macronova”) due to the decay of **heavy radioactive species** produced by the *r*-process and ejected during the merger that is expected to provide a source of heating and radiation (Li and Paczynski 1998; Rosswog, 2005; Metzger et al., 2010).



Follow-up strategy



Follow-up strategy



The GW era – O1 & O2



Sept 2015 – Jan 2016: LVC O1 science run
Nov 2016 – Aug 2017: LVC O2 science run



Event	m_1/M_\odot	m_2/M_\odot	M/M_\odot	χ_{eff}	M_f/M_\odot	a_f	$E_{\text{rad}}/(M_\odot c^2)$	$\ell_{\text{peak}}/(\text{erg s}^{-1})$	d_L/Mpc	z	$\Delta\Omega/\text{deg}^2$
GW150914	$35.6^{+4.8}_{-3.0}$	$30.6^{+3.0}_{-4.4}$	$28.6^{+1.6}_{-1.5}$	$-0.01^{+0.12}_{-0.13}$	$63.1^{+3.3}_{-3.0}$	$0.69^{+0.05}_{-0.04}$	$3.1^{+0.4}_{-0.4}$	$3.6^{+0.4}_{-0.4} \times 10^{56}$	430^{+150}_{-170}	$0.09^{+0.03}_{-0.03}$	180
GW151012	$23.3^{+14.0}_{-5.5}$	$13.6^{+4.1}_{-4.8}$	$15.2^{+2.0}_{-1.1}$	$0.04^{+0.28}_{-0.19}$	$35.7^{+9.9}_{-3.8}$	$0.67^{+0.13}_{-0.11}$	$1.5^{+0.5}_{-0.5}$	$3.2^{+0.8}_{-1.7} \times 10^{56}$	1060^{+540}_{-480}	$0.21^{+0.09}_{-0.09}$	1555
GW151226	$13.7^{+8.8}_{-3.2}$	$7.7^{+2.2}_{-2.6}$	$8.9^{+0.3}_{-0.3}$	$0.18^{+0.20}_{-0.12}$	$20.5^{+6.4}_{-1.5}$	$0.74^{+0.07}_{-0.05}$	$1.0^{+0.1}_{-0.2}$	$3.4^{+0.7}_{-1.7} \times 10^{56}$	440^{+180}_{-190}	$0.09^{+0.04}_{-0.04}$	1033
GW170104	$31.0^{+7.2}_{-5.6}$	$20.1^{+4.9}_{-4.5}$	$21.5^{+2.1}_{-1.7}$	$-0.04^{+0.17}_{-0.20}$	$49.1^{+5.2}_{-3.9}$	$0.66^{+0.08}_{-0.10}$	$2.2^{+0.5}_{-0.5}$	$3.3^{+0.6}_{-0.9} \times 10^{56}$	960^{+430}_{-410}	$0.19^{+0.07}_{-0.08}$	924
GW170608	$10.9^{+5.3}_{-1.7}$	$7.6^{+1.3}_{-2.1}$	$7.9^{+0.2}_{-0.2}$	$0.03^{+0.19}_{-0.07}$	$17.8^{+3.2}_{-0.7}$	$0.69^{+0.04}_{-0.04}$	$0.9^{+0.05}_{-0.1}$	$3.5^{+0.4}_{-1.3} \times 10^{56}$	320^{+120}_{-110}	$0.07^{+0.02}_{-0.02}$	396
GW170729	$50.6^{+16.6}_{-10.2}$	$34.3^{+9.1}_{-10.1}$	$35.7^{+6.5}_{-4.7}$	$0.36^{+0.21}_{-0.25}$	$80.3^{+14.6}_{-10.2}$	$0.81^{+0.07}_{-0.13}$	$4.8^{+1.7}_{-1.7}$	$4.2^{+0.9}_{-1.5} \times 10^{56}$	2750^{+1350}_{-1320}	$0.48^{+0.19}_{-0.20}$	1033
GW170809	$35.2^{+8.3}_{-6.0}$	$23.8^{+5.2}_{-5.1}$	$25.0^{+2.1}_{-1.6}$	$0.07^{+0.16}_{-0.16}$	$56.4^{+5.2}_{-3.7}$	$0.70^{+0.08}_{-0.09}$	$2.7^{+0.6}_{-0.6}$	$3.5^{+0.6}_{-0.9} \times 10^{56}$	990^{+320}_{-380}	$0.20^{+0.05}_{-0.07}$	340
GW170814	$30.7^{+5.7}_{-3.0}$	$25.3^{+2.9}_{-4.1}$	$24.2^{+1.4}_{-1.1}$	$0.07^{+0.12}_{-0.11}$	$53.4^{+3.2}_{-2.4}$	$0.72^{+0.07}_{-0.05}$	$2.7^{+0.4}_{-0.3}$	$3.7^{+0.4}_{-0.5} \times 10^{56}$	580^{+160}_{-210}	$0.12^{+0.03}_{-0.04}$	87
GW170817	$1.46^{+0.12}_{-0.10}$	$1.27^{+0.09}_{-0.09}$	$1.186^{+0.001}_{-0.001}$	$0.00^{+0.02}_{-0.01}$	≤ 2.8	≤ 0.89	≥ 0.04	$\geq 0.1 \times 10^{56}$	40^{+10}_{-10}	$0.01^{+0.00}_{-0.00}$	16
GW170818	$35.5^{+7.5}_{-4.7}$	$26.8^{+4.3}_{-5.2}$	$26.7^{+2.1}_{-1.7}$	$-0.09^{+0.18}_{-0.21}$	$59.8^{+4.8}_{-3.8}$	$0.67^{+0.07}_{-0.08}$	$2.7^{+0.5}_{-0.5}$	$3.4^{+0.5}_{-0.7} \times 10^{56}$	1020^{+430}_{-360}	$0.20^{+0.07}_{-0.07}$	39
GW170823	$39.6^{+10.0}_{-6.6}$	$29.4^{+6.3}_{-7.1}$	$29.3^{+4.2}_{-3.2}$	$0.08^{+0.20}_{-0.22}$	$65.6^{+9.4}_{-6.6}$	$0.71^{+0.08}_{-0.10}$	$3.3^{+0.9}_{-0.8}$	$3.6^{+0.6}_{-0.9} \times 10^{56}$	1850^{+840}_{-840}	$0.34^{+0.13}_{-0.14}$	1651



The GW era – O1 & O2



Sept 2015 – Jan 2016: LVC O1 science run
Nov 2016 – Aug 2017: LVC O2 science run



Event	m_1/M_\odot	m_2/M_\odot	M/M_\odot	χ_{eff}	M_f/M_\odot	a_f	$E_{\text{rad}}/(M_\odot c^2)$	$\ell_{\text{peak}}/(\text{erg s}^{-1})$	d_L/Mpc	z	$\Delta\Omega/\text{deg}^2$
GW150914	$35.6^{+4.8}_{-3.0}$	$30.6^{+3.0}_{-4.4}$	$28.6^{+1.6}_{-1.5}$	$-0.01^{+0.12}_{-0.13}$	$63.1^{+3.3}_{-3.0}$	$0.69^{+0.05}_{-0.04}$	$3.1^{+0.4}_{-0.4}$	$3.6^{+0.4}_{-0.4} \times 10^{56}$	430^{+150}_{-170}	$0.09^{+0.03}_{-0.03}$	180
GW151012	$23.3^{+14.0}_{-5.5}$	$13.6^{+4.1}_{-4.8}$	$15.2^{+2.0}_{-1.1}$	$0.04^{+0.28}_{-0.19}$	$35.7^{+9.9}_{-3.8}$	$0.67^{+0.13}_{-0.11}$	$1.5^{+0.5}_{-0.5}$	$3.2^{+0.8}_{-1.7} \times 10^{56}$	1060^{+540}_{-480}	$0.21^{+0.09}_{-0.09}$	1555
GW151226	$13.7^{+8.8}_{-3.2}$	$7.7^{+2.2}_{-2.6}$	$8.9^{+0.3}_{-0.3}$	$0.18^{+0.20}_{-0.12}$	$20.5^{+6.4}_{-1.5}$	$0.74^{+0.07}_{-0.05}$	$1.0^{+0.1}_{-0.2}$	$3.4^{+0.7}_{-1.7} \times 10^{56}$	440^{+180}_{-190}	$0.09^{+0.04}_{-0.04}$	1033
GW170104	$31.0^{+7.2}_{-5.6}$	$20.1^{+4.9}_{-4.5}$	$21.5^{+2.1}_{-1.7}$	$-0.04^{+0.17}_{-0.20}$	$49.1^{+5.2}_{-3.9}$	$0.66^{+0.08}_{-0.10}$	$2.2^{+0.5}_{-0.5}$	$3.3^{+0.6}_{-0.9} \times 10^{56}$	960^{+430}_{-410}	$0.19^{+0.07}_{-0.08}$	924
GW170608	$10.9^{+5.3}_{-1.7}$	$7.6^{+1.3}_{-2.1}$	$7.9^{+0.2}_{-0.2}$	$0.03^{+0.19}_{-0.07}$	$17.8^{+3.2}_{-0.7}$	$0.69^{+0.04}_{-0.04}$	$0.9^{+0.05}_{-0.1}$	$3.5^{+0.4}_{-1.3} \times 10^{56}$	320^{+120}_{-110}	$0.07^{+0.02}_{-0.02}$	396
GW170729	$50.6^{+16.6}_{-10.2}$	$34.3^{+9.1}_{-10.1}$	$35.7^{+6.5}_{-4.7}$	$0.36^{+0.21}_{-0.25}$	$80.3^{+14.6}_{-10.2}$	$0.81^{+0.07}_{-0.13}$	$4.8^{+1.7}_{-1.7}$	$4.2^{+0.9}_{-1.5} \times 10^{56}$	2750^{+1350}_{-1320}	$0.48^{+0.19}_{-0.20}$	1033
GW170809	$35.2^{+8.3}_{-6.0}$	$23.8^{+5.2}_{-5.1}$	$25.0^{+2.1}_{-1.6}$	$0.07^{+0.16}_{-0.16}$	$56.4^{+5.2}_{-3.7}$	$0.70^{+0.08}_{-0.09}$	$2.7^{+0.6}_{-0.6}$	$3.5^{+0.6}_{-0.9} \times 10^{56}$	990^{+320}_{-380}	$0.20^{+0.05}_{-0.07}$	340
GW170814	$30.7^{+5.7}_{-3.0}$	$25.3^{+2.9}_{-4.1}$	$24.2^{+1.4}_{-1.1}$	$0.07^{+0.12}_{-0.11}$	$53.4^{+3.2}_{-2.4}$	$0.72^{+0.07}_{-0.05}$	$2.7^{+0.4}_{-0.3}$	$3.7^{+0.4}_{-0.5} \times 10^{56}$	580^{+160}_{-210}	$0.12^{+0.03}_{-0.04}$	87
GW170817	$1.46^{+0.12}_{-0.10}$	$1.27^{+0.09}_{-0.09}$	$1.186^{+0.001}_{-0.001}$	$0.00^{+0.02}_{-0.01}$	≤ 2.8	≤ 0.89	≥ 0.04	$\geq 0.1 \times 10^{56}$	40^{+10}_{-10}	$0.01^{+0.00}_{-0.00}$	16
GW170818	$35.5^{+7.5}_{-4.7}$	$26.8^{+4.3}_{-5.2}$	$26.7^{+2.1}_{-1.7}$	$-0.09^{+0.18}_{-0.21}$	$59.8^{+4.8}_{-3.8}$	$0.67^{+0.07}_{-0.08}$	$2.7^{+0.5}_{-0.5}$	$3.4^{+0.5}_{-0.7} \times 10^{56}$	1020^{+430}_{-360}	$0.20^{+0.07}_{-0.07}$	39
GW170823	$39.6^{+10.0}_{-6.6}$	$29.4^{+6.3}_{-7.1}$	$29.3^{+4.2}_{-3.2}$	$0.08^{+0.20}_{-0.22}$	$65.6^{+9.4}_{-6.6}$	$0.71^{+0.08}_{-0.10}$	$3.3^{+0.9}_{-0.8}$	$3.6^{+0.6}_{-0.9} \times 10^{56}$	1850^{+840}_{-840}	$0.34^{+0.13}_{-0.14}$	1651



The GW era – O1 & O2



Sept 2015 – Jan 2016: LVC O1 science run
Nov 2016 – Aug 2017: LVC O2 science run



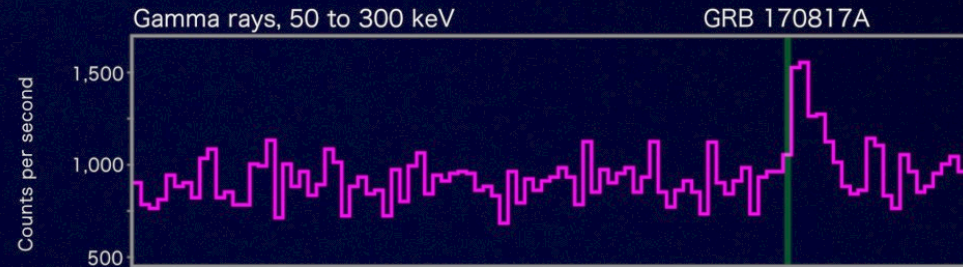
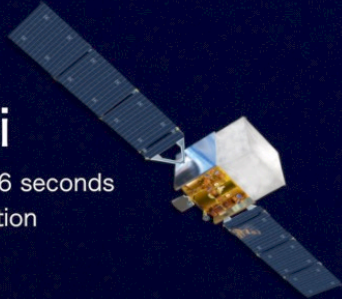
Event	m_1/M_\odot	m_2/M_\odot	M/M_\odot	χ_{eff}	M_f/M_\odot	a_f	$E_{\text{rad}}/(M_\odot c^2)$	$\ell_{\text{peak}}/(\text{erg s}^{-1})$	d_L/Mpc	z	$\Delta\Omega/\text{deg}^2$
GW150914	$35.6^{+4.8}_{-3.0}$	$30.6^{+3.0}_{-4.4}$	$28.6^{+1.6}_{-1.5}$	$-0.01^{+0.12}_{-0.13}$	$63.1^{+3.3}_{-3.0}$	$0.69^{+0.05}_{-0.04}$	$3.1^{+0.4}_{-0.4}$	$3.6^{+0.4}_{-0.4} \times 10^{56}$	430^{+150}_{-170}	$0.09^{+0.03}_{-0.03}$	180
GW151012	$23.3^{+14.0}_{-5.5}$	$13.6^{+4.1}_{-4.8}$	$15.2^{+2.0}_{-1.1}$	$0.04^{+0.28}_{-0.19}$	$35.7^{+9.9}_{-3.8}$	$0.67^{+0.13}_{-0.11}$	$1.5^{+0.5}_{-0.5}$	$3.2^{+0.8}_{-1.7} \times 10^{56}$	1060^{+540}_{-480}	$0.21^{+0.09}_{-0.09}$	1555
GW151226	$13.7^{+8.8}_{-3.2}$	$7.7^{+2.2}_{-2.6}$	$8.9^{+0.3}_{-0.3}$	$0.18^{+0.20}_{-0.12}$	$20.5^{+6.4}_{-1.5}$	$0.74^{+0.07}_{-0.05}$	$1.0^{+0.1}_{-0.2}$	$3.4^{+0.7}_{-1.7} \times 10^{56}$	440^{+180}_{-190}	$0.09^{+0.04}_{-0.04}$	1033
GW170104	$31.0^{+7.2}_{-5.6}$	$20.1^{+4.9}_{-4.5}$	$21.5^{+2.1}_{-1.7}$	$-0.04^{+0.17}_{-0.20}$	$49.1^{+5.2}_{-3.9}$	$0.66^{+0.08}_{-0.10}$	$2.2^{+0.5}_{-0.5}$	$3.3^{+0.6}_{-0.9} \times 10^{56}$	960^{+430}_{-410}	$0.19^{+0.07}_{-0.08}$	924
GW170608	$10.9^{+5.3}_{-1.7}$	$7.6^{+1.3}_{-2.1}$	$7.9^{+0.2}_{-0.2}$	$0.03^{+0.19}_{-0.07}$	$17.8^{+3.2}_{-0.7}$	$0.69^{+0.04}_{-0.04}$	$0.9^{+0.05}_{-0.1}$	$3.5^{+0.4}_{-1.3} \times 10^{56}$	320^{+120}_{-110}	$0.07^{+0.02}_{-0.02}$	396
GW170729	$50.6^{+16.6}_{-10.2}$	$34.3^{+9.1}_{-10.1}$	$35.7^{+6.5}_{-4.7}$	$0.36^{+0.21}_{-0.25}$	$80.3^{+14.6}_{-10.2}$	$0.81^{+0.07}_{-0.13}$	$4.8^{+1.7}_{-1.7}$	$4.2^{+0.9}_{-1.5} \times 10^{56}$	2750^{+1350}_{-1320}	$0.48^{+0.19}_{-0.20}$	1033
GW170809	$35.2^{+8.3}_{-6.0}$	$23.8^{+5.2}_{-5.1}$	$25.0^{+2.1}_{-1.6}$	$0.07^{+0.16}_{-0.16}$	$56.4^{+5.2}_{-3.7}$	$0.70^{+0.08}_{-0.09}$	$2.7^{+0.6}_{-0.6}$	$3.5^{+0.6}_{-0.9} \times 10^{56}$	990^{+320}_{-380}	$0.20^{+0.05}_{-0.07}$	340
GW170814	$30.7^{+5.7}_{-3.0}$	$25.3^{+2.9}_{-4.1}$	$24.2^{+1.4}_{-1.1}$	$0.07^{+0.12}_{-0.11}$	$53.4^{+3.2}_{-2.4}$	$0.72^{+0.07}_{-0.05}$	$2.7^{+0.4}_{-0.3}$	$3.7^{+0.4}_{-0.5} \times 10^{56}$	580^{+160}_{-210}	$0.12^{+0.03}_{-0.04}$	87
GW170817	$1.46^{+0.12}_{-0.10}$	$1.27^{+0.09}_{-0.09}$	$1.186^{+0.001}_{-0.001}$	$0.00^{+0.02}_{-0.01}$	≤ 2.8	≤ 0.89	≥ 0.04	$\geq 0.1 \times 10^{56}$	40^{+10}_{-10}	$0.01^{+0.00}_{-0.00}$	16
GW170818	$35.5^{+7.5}_{-4.7}$	$26.8^{+4.3}_{-5.2}$	$26.7^{+2.1}_{-1.7}$	$-0.09^{+0.18}_{-0.21}$	$59.8^{+4.8}_{-3.8}$	$0.67^{+0.07}_{-0.08}$	$2.7^{+0.5}_{-0.5}$	$3.4^{+0.5}_{-0.7} \times 10^{56}$	1020^{+430}_{-360}	$0.20^{+0.07}_{-0.07}$	39
GW170823	$39.6^{+10.0}_{-6.6}$	$29.4^{+6.3}_{-7.1}$	$29.3^{+4.2}_{-3.2}$	$0.08^{+0.20}_{-0.22}$	$65.6^{+9.4}_{-6.6}$	$0.71^{+0.08}_{-0.10}$	$3.3^{+0.9}_{-0.8}$	$3.6^{+0.6}_{-0.9} \times 10^{56}$	1850^{+840}_{-840}	$0.34^{+0.13}_{-0.14}$	1651



GW 170817 & GRB 170817A

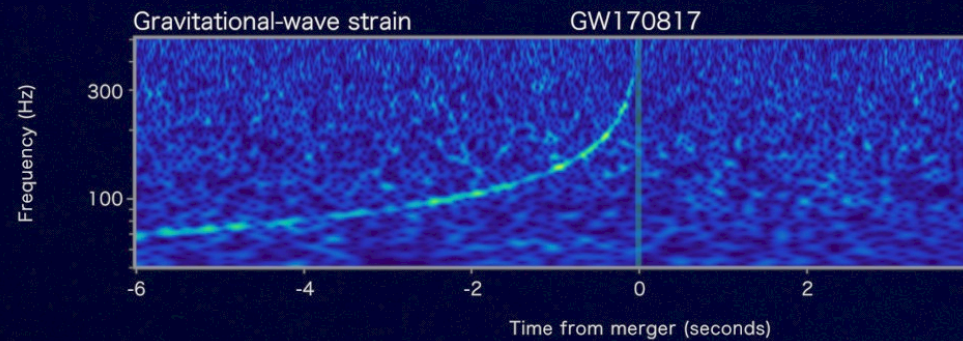
Fermi

Reported 16 seconds
after detection



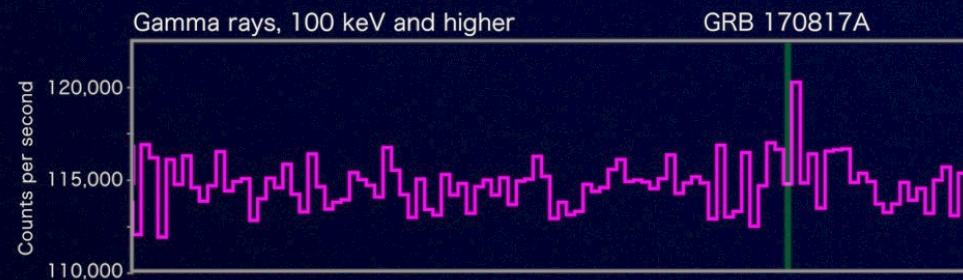
LIGO-Virgo

Reported 27 minutes after detection



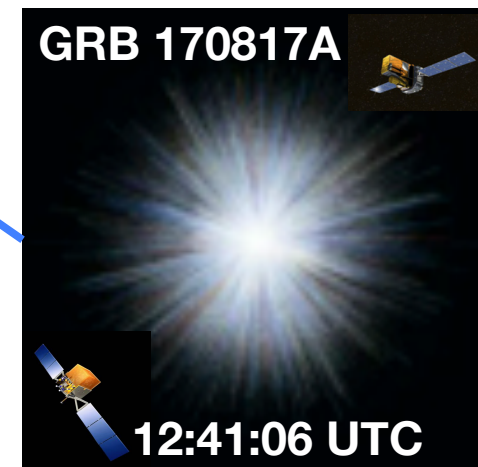
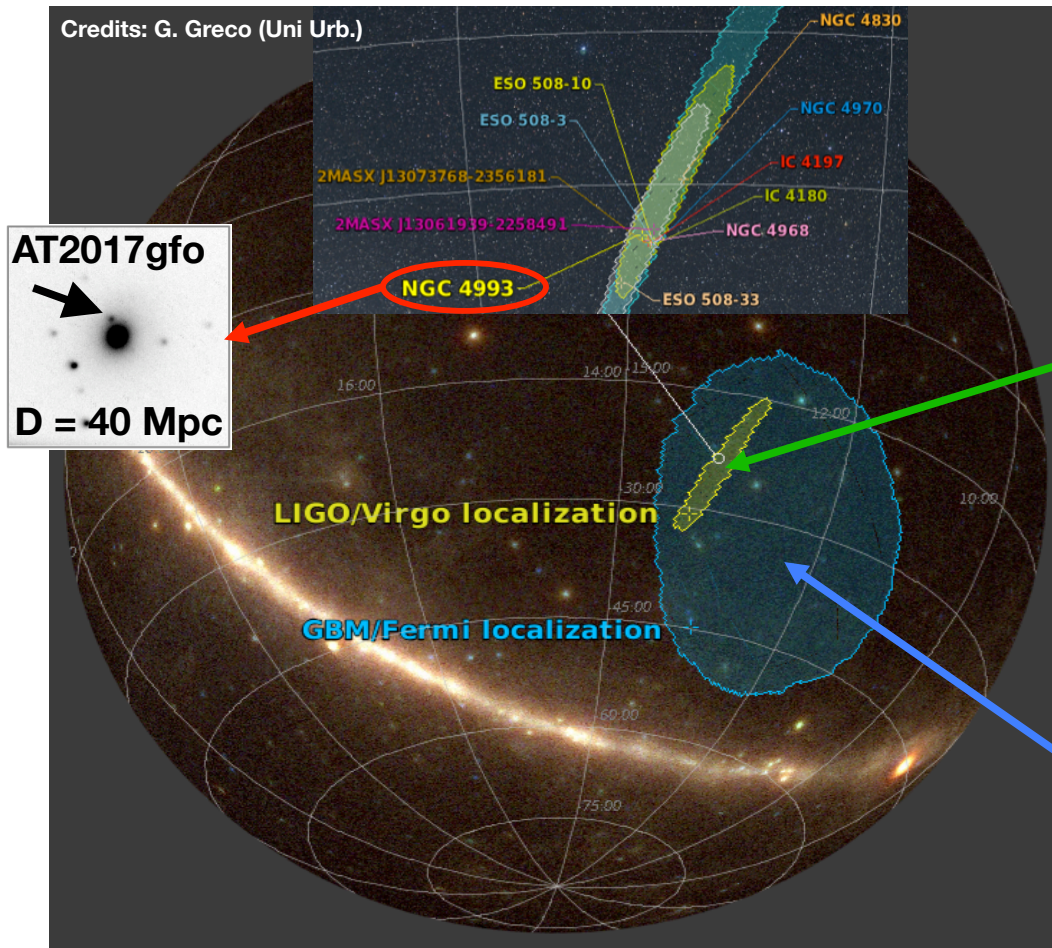
INTEGRAL

Reported 66 minutes
after detection



Abbott+17; Goldstein+17; Savchenko+17

GW 170817 / GRB 170817A / AT2017gfo



PRL 119, 161101 (2017) Selected for a Viewpoint in *Physics* PHYSICAL REVIEW LETTERS week ending 20 OCTOBER 2017

GW170817: Observation of Gravitational Waves from a Binary Neutron Star Inspiral

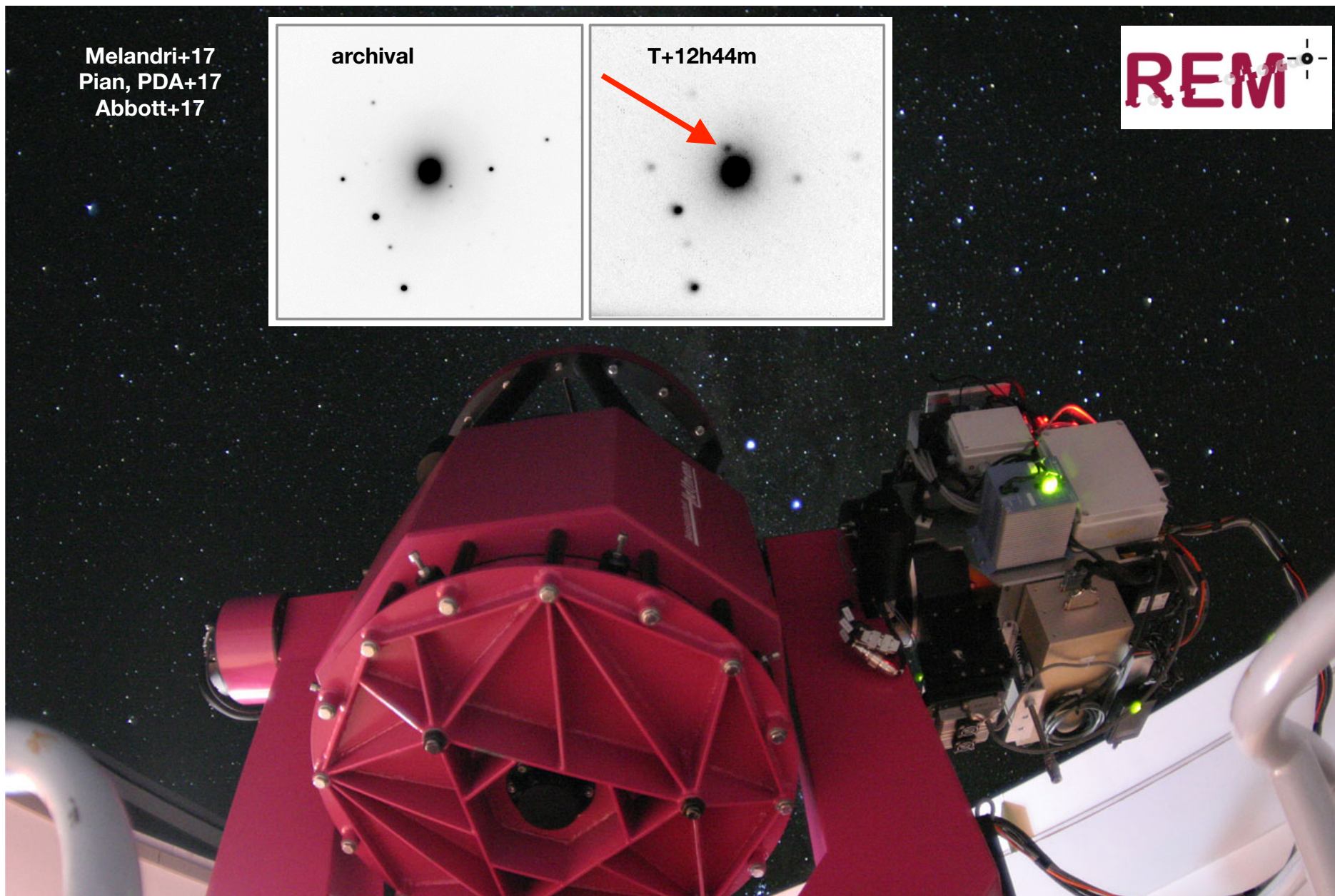
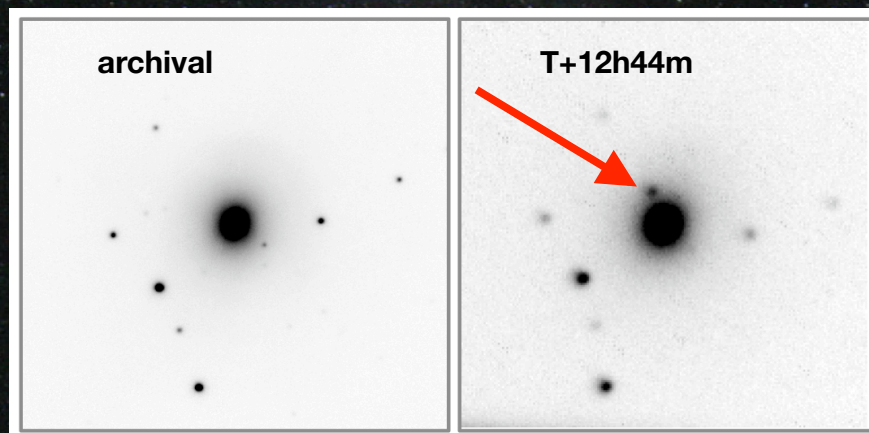
B. P. Abbott *et al.**

(LIGO Scientific Collaboration and Virgo Collaboration)

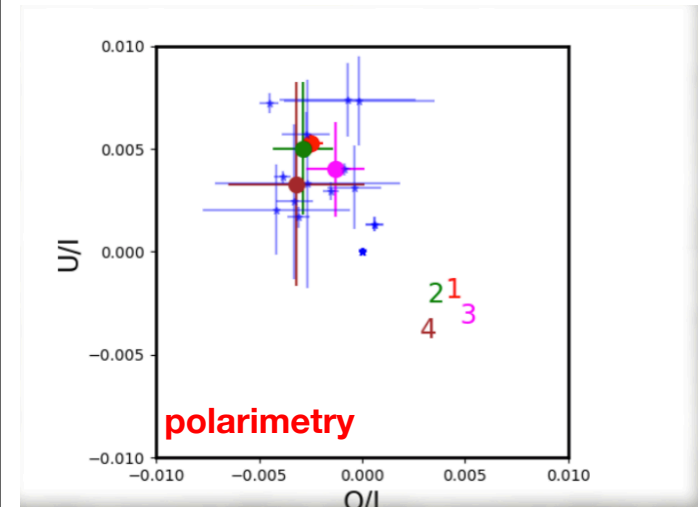
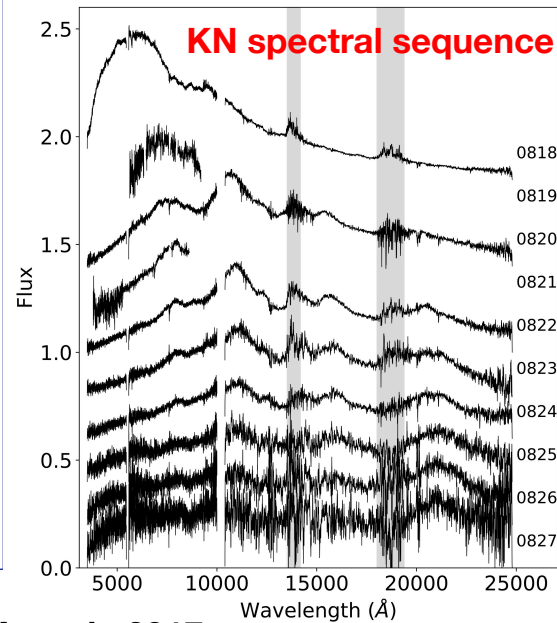
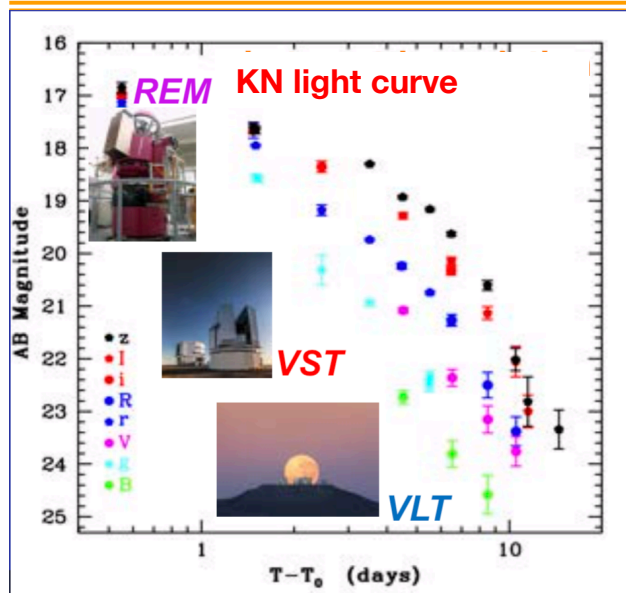
(Received 26 September 2017; revised manuscript received 2 October 2017; published 16 October 2017)

GW 170817 / GRB 170817A / AT2017gfo

Melandri+17
Pian, PDA+17
Abbott+17



GW 170817 / GRB 170817A / AT2017gfo



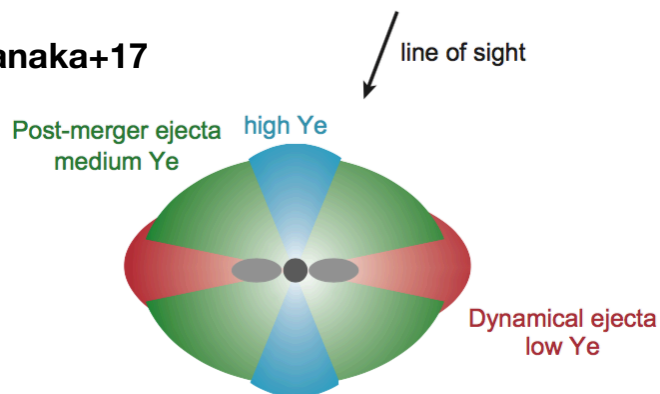
Pian, PDA et al., 2017

(see also Arcavi+17; Coulter+17; Evans+17; Lipunov+17; Smartt+17; Soares-Santos+17; Tanvir+17; Valenti+17 and many others)

Covino et al., 2017

Full characterization of the KN properties

Tanaka+17

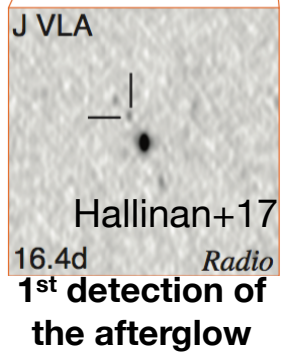
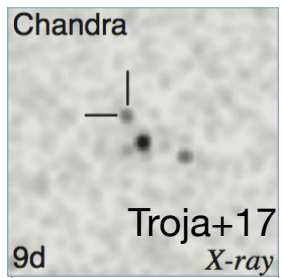


Three components Kilonova model with different velocity, composition and electron (proton) fraction (low Y_e : lanthanide-rich; high Y_e : lanthanide-poor)

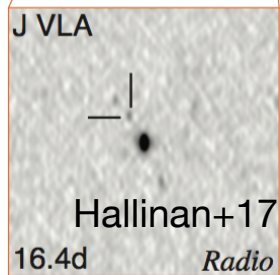
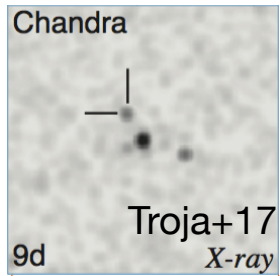
0.03-0.05 M_{Sun} ejected mass

Fast moving dynamical ejecta (0.2c) + slower wind (0.05c)

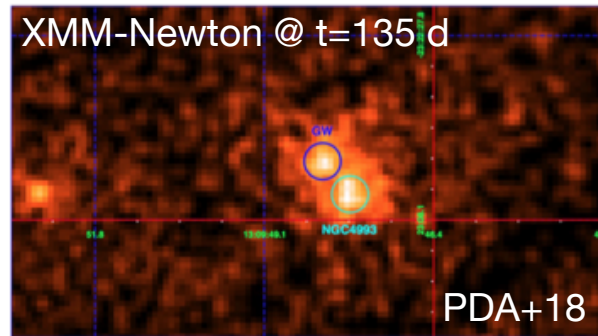
GW 170817 / AT2017gfo / GRB 170817A



GW 170817 / AT2017gfo / GRB 170817A

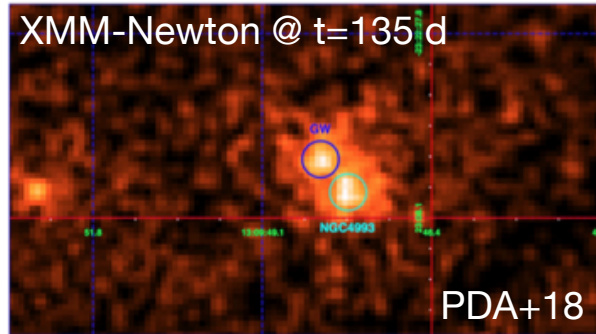
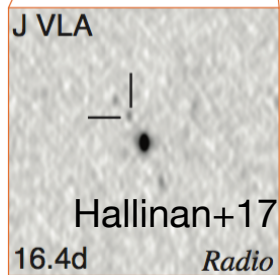
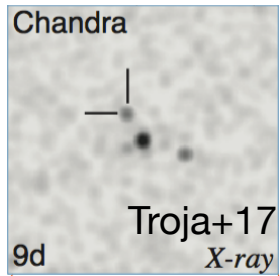


**1st detection of
the afterglow**

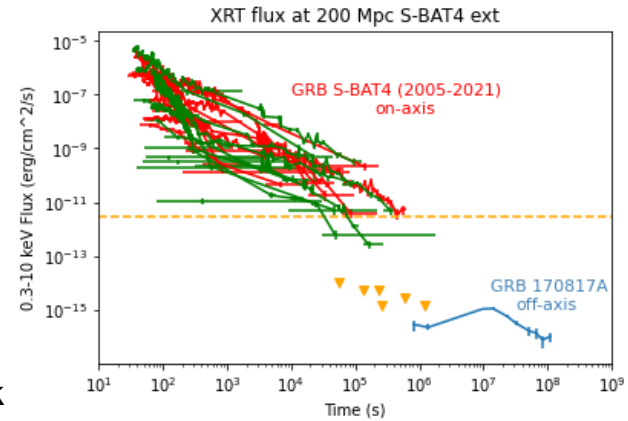


detection of the afterglow at the peak

GW 170817 / AT2017gfo / GRB 170817A



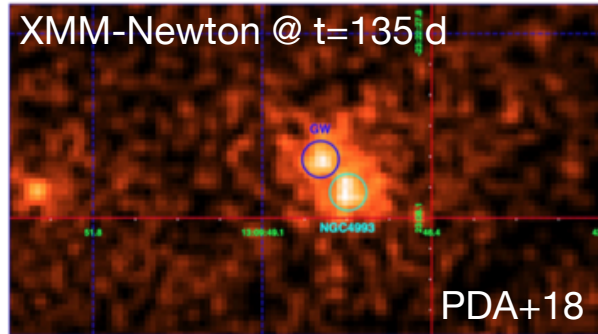
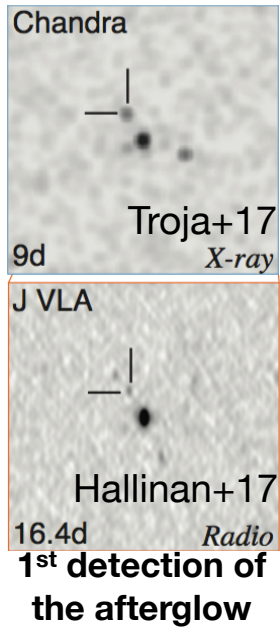
detection of the afterglow at the peak



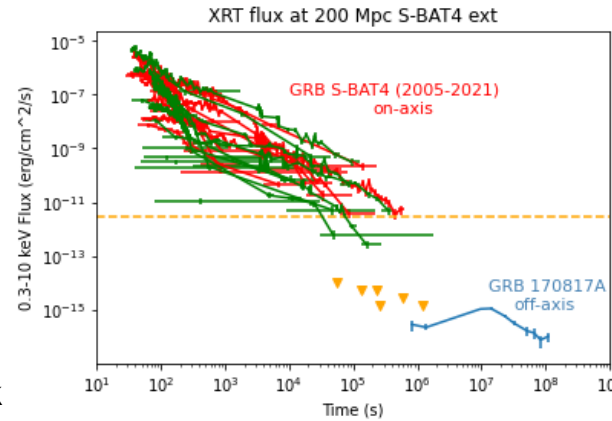
Michela Di Natolo (Bachelor student)
see also Duan+19; Salafia+19

1st detection of the afterglow

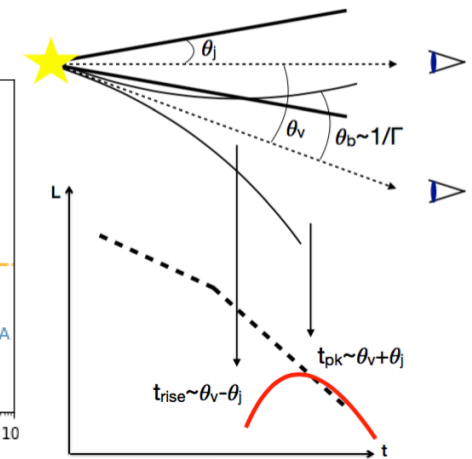
GW 170817 / AT2017gfo / GRB 170817A



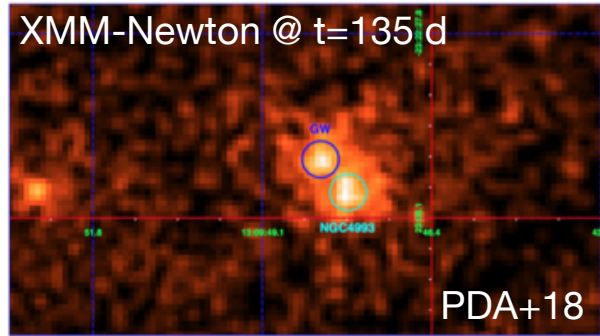
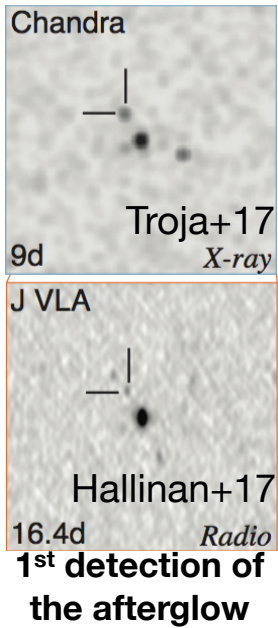
detection of the afterglow at the peak



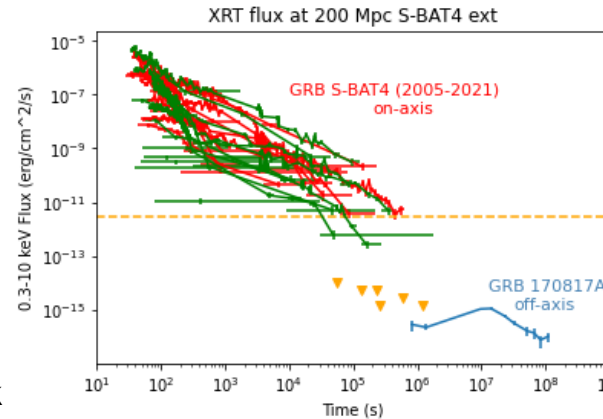
Michela Di Natolo (Bachelor student)
see also Duan+19; Salafia+19



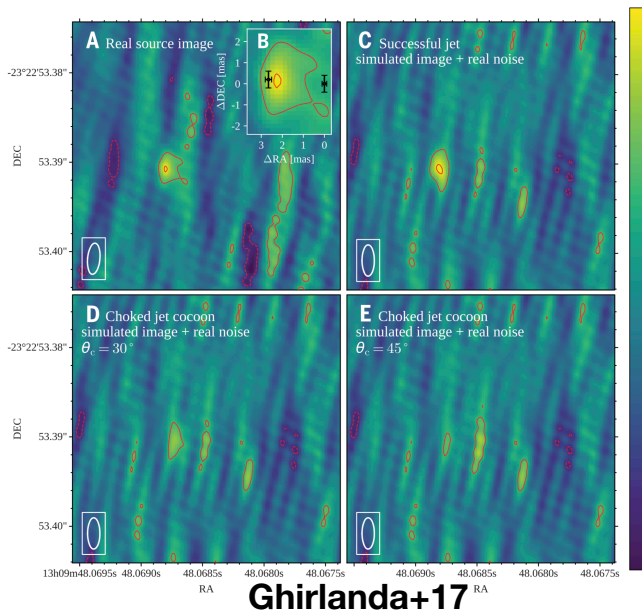
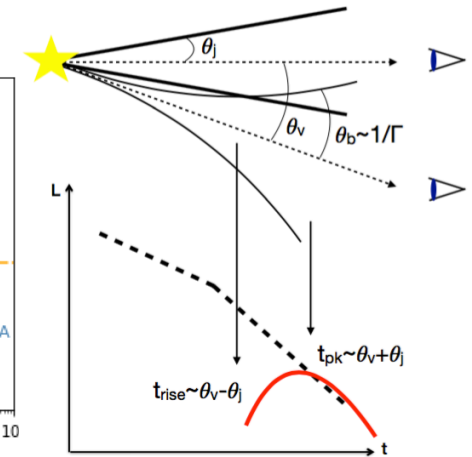
GW 170817 / AT2017gfo / GRB 170817A



detection of the afterglow at the peak

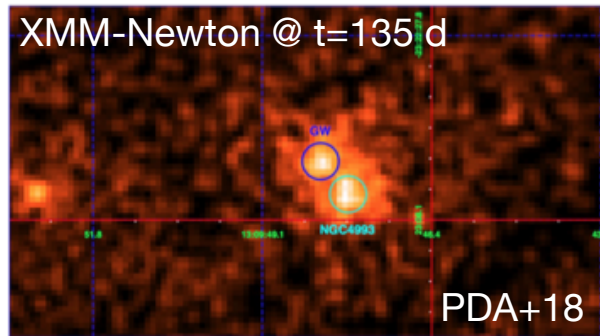
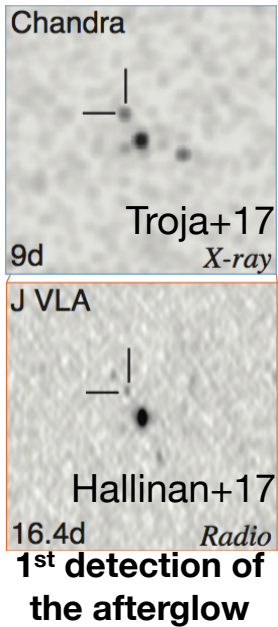


Michela Di Natolo (Bachelor student)
see also Duan+19; Salafia+19

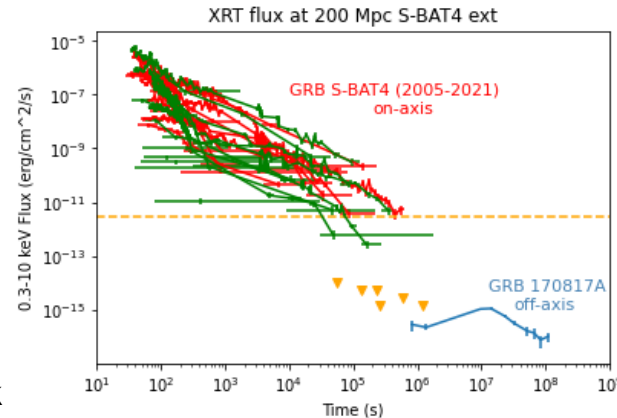


The radio afterglow is detected with an angular size < 2 mas in VLBI data obtained ~ 207 d after the merger. Evidence for superluminal motion is also found measuring an angular offset between T+75 d and T+235 d.

GW 170817 / AT2017gfo / GRB 170817A

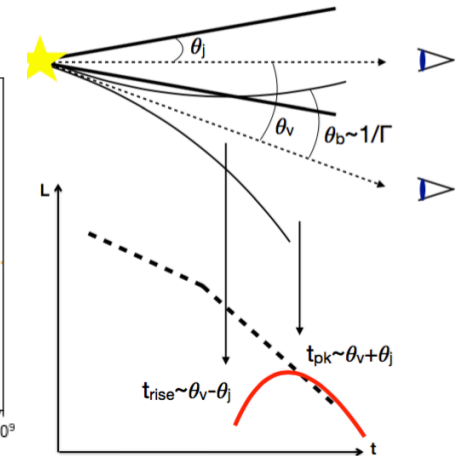


detection of the afterglow at the peak

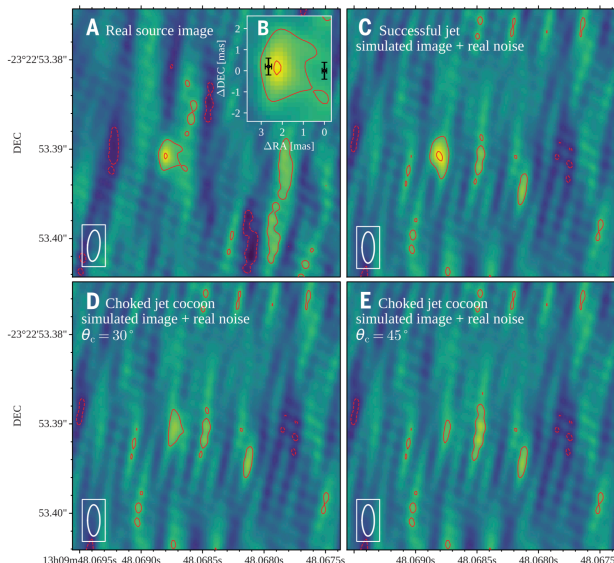


Michela Di Natolo (Bachelor student)

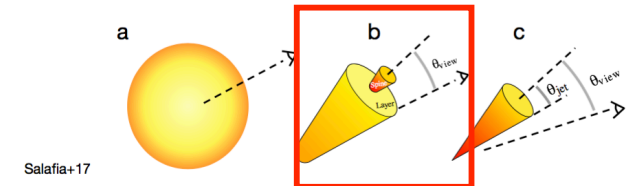
see also Duan+19; Salafia+19



Full characterization of the GRB properties: evidence for a structured jet



Ghirlanda+17

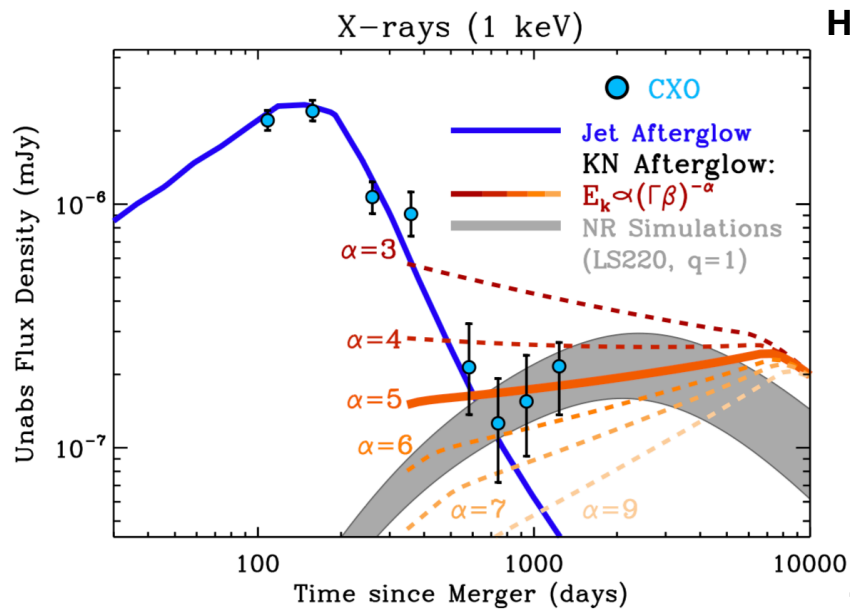


The radio afterglow is detected with an angular size < 2 mas in VLBI data obtained ~ 207 d after the merger. Evidence for superluminal motion is also found measuring an angular offset between T+75 d and T+235 d.

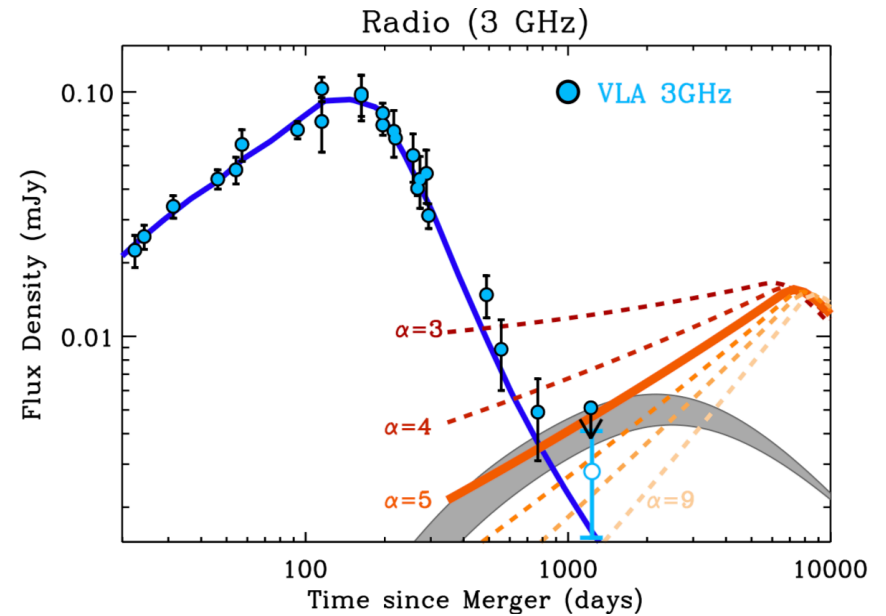
These findings, together with the afterglow light curve modelling, support the **structured jet** model. Fit to the data and numerical simulations are in agreement with the scenario of a structured jet with a relativistic core with $\theta_{\text{jet}} < 5$ deg and $\theta_{\text{view}} \sim 20$ deg.

Alexander+17,18; PDA+18; Dobie+18; Fong+19; Haggard+17; Hallinan+17; Hajela+19; Margutti+17,18; Mooley+18a,b; Reasmi+18; Ruan+18; Troja+18a,b, 19,20; Ghirlanda+19; Piro+19; Margutti & Chornock 21 and many others

GRB170817A: still detected after years



Hajela+21

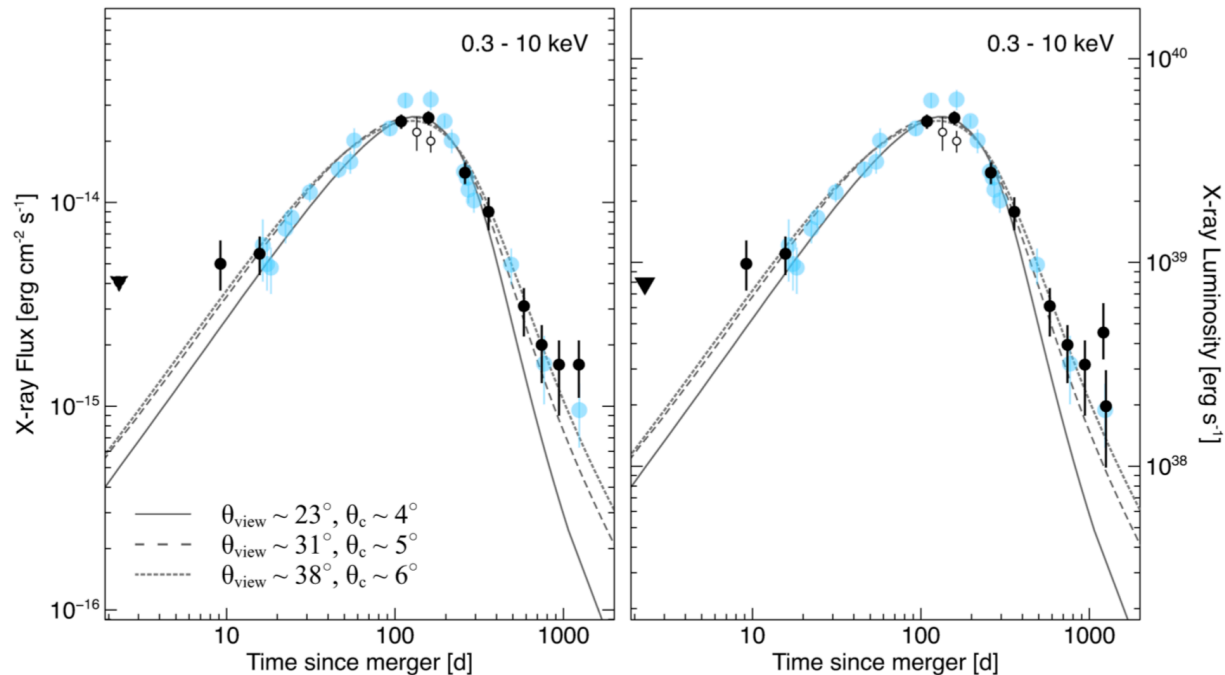


Troja+21

KN afterglow?

Accretion on compact remnant?

Magnetar?



O1 & O2: lessons learned

O1 & O2: lessons learned



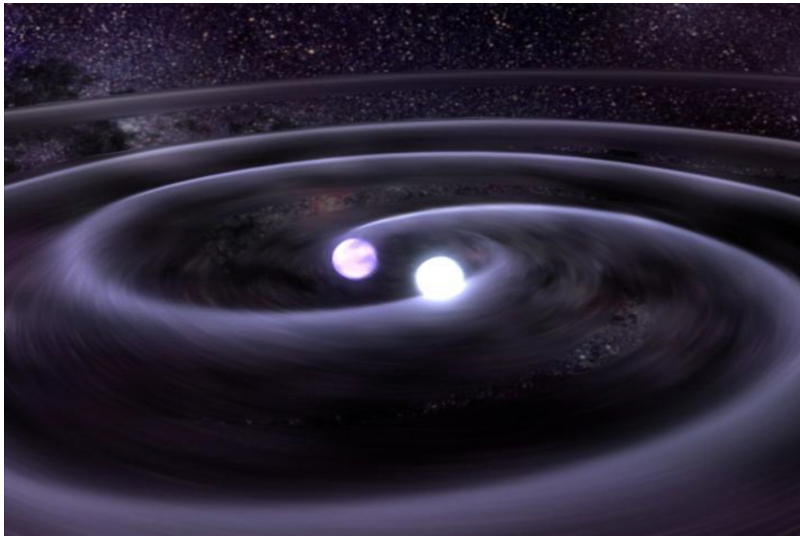
O1 & O2: lessons learned



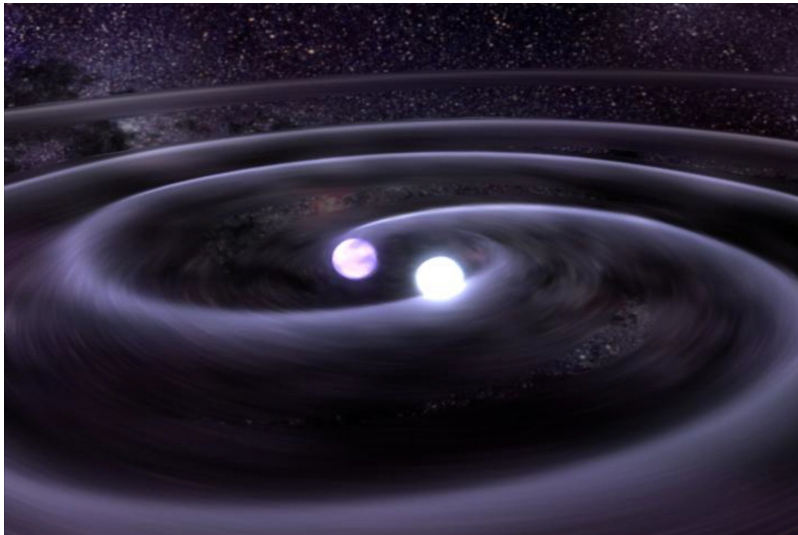
O1 & O2: lessons learned



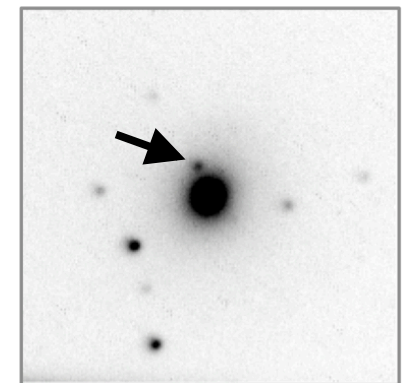
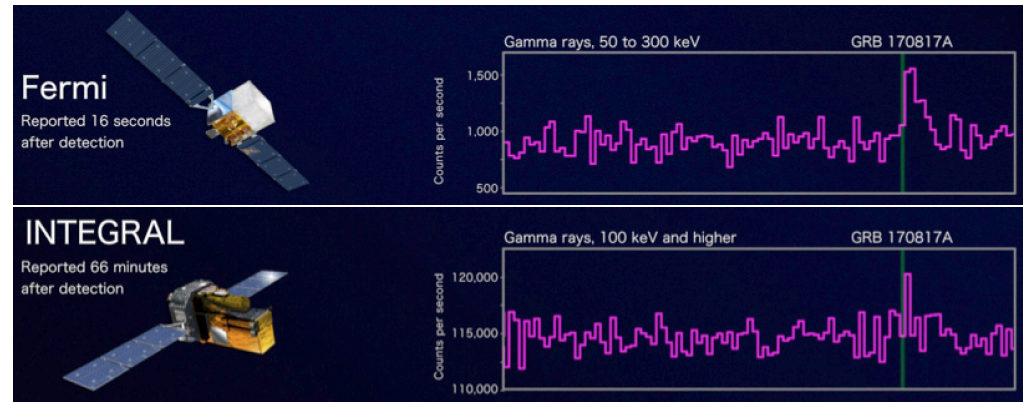
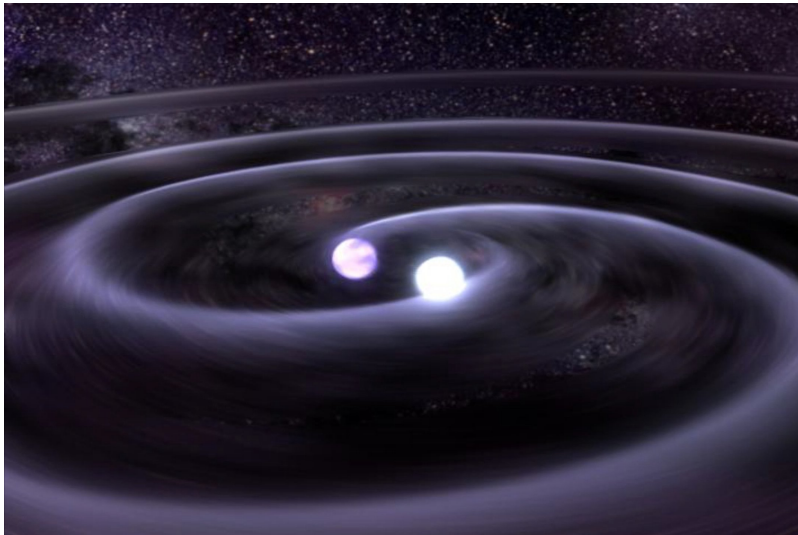
O1 & O2: lessons learned



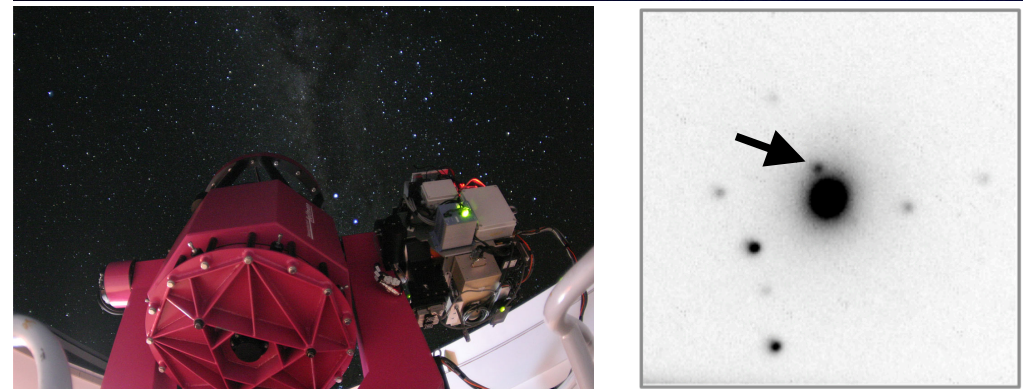
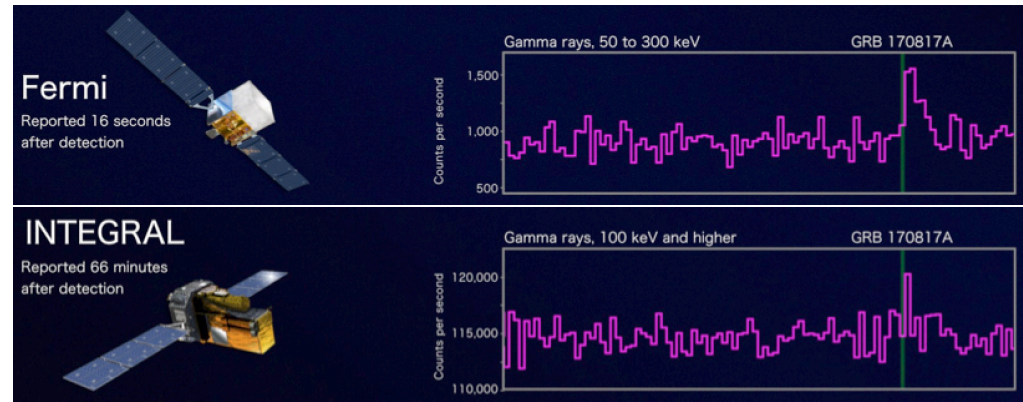
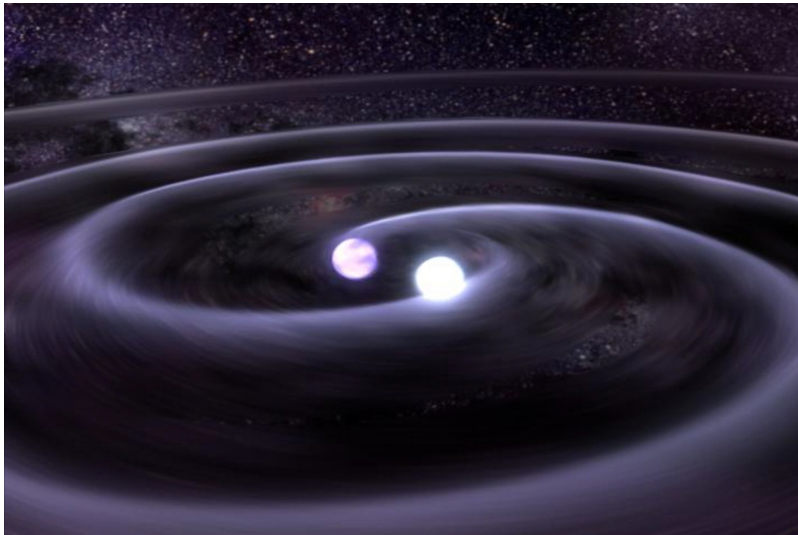
O1 & O2: lessons learned



O1 & O2: lessons learned



O1 & O2: lessons learned



The Multi-Messenger era

- **GW 170717 / GRB 170817A / AT2017gfo results:**

- Definition and consolidation of successful follow-up strategies
- First GW EM counterpart (at all wavelengths)
- First unambiguous observational evidence for a kilonova
- Evidence for kilonovae as a heavy elements factory
- `Smoking gun' for short GRB progenitors
- Clues on short GRB outflow geometry and properties: first evidence for a structured jet
- Direct EM distance determination (cosmology)

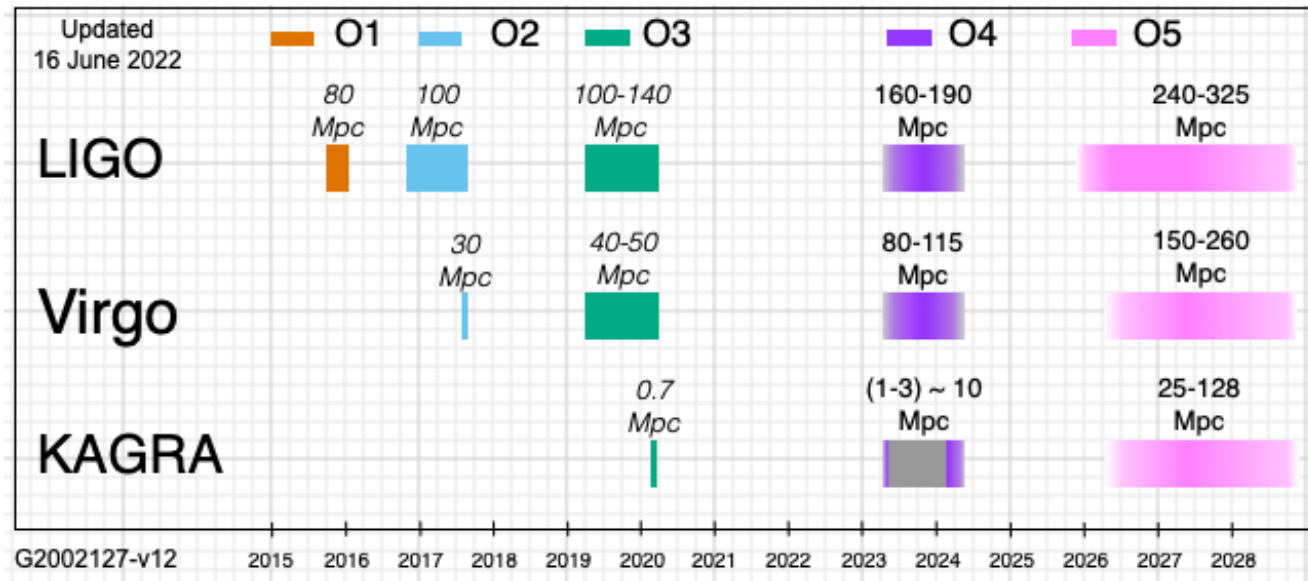
- **Still a number of open issues**

- what about BH-NS EM counterparts?
- what is the origin of the blue KN component?
- are KNe associated to every short GRB?
- how to unveil the nature of the NS-NS remnant?
- (...)

- **Scientific perspectives and opportunities:**

- Characterize the counterparts of NS-NS / NS-BH mergers
- Determine the yield of heavy elements from KNe
- Study the jet structure, rate and energetics of short GRBs
- Characterize the environment & probe into the binary evolutionary channels
- Direct EM distance determinations on a sample of events
- The unknown

The GW era – O3

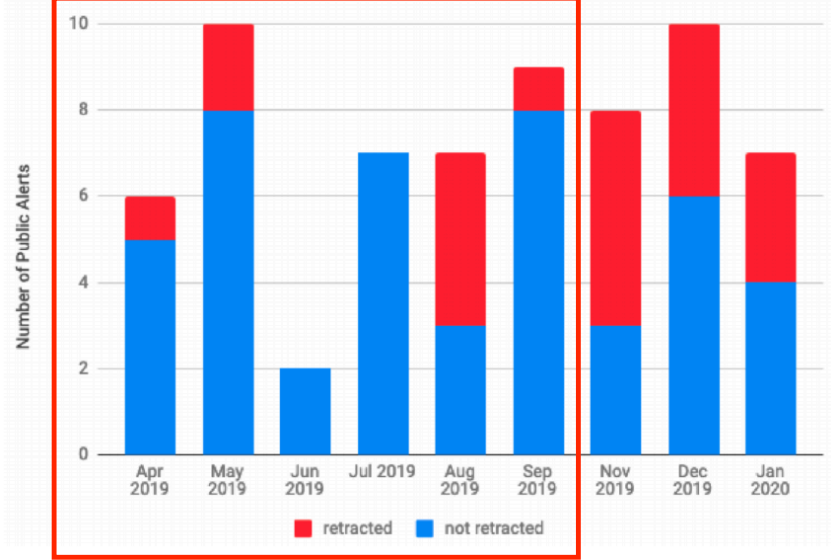


The GW era – O3a



Event	M (M_{\odot})	\mathcal{M} (M_{\odot})	m_1 (M_{\odot})	m_2 (M_{\odot})	χ_{eff}	D_L (Gpc)	z	M_f (M_{\odot})	χ_f	$\Delta\Omega$ (deg 2)	SNR
GW190408_181802	43.0 $^{+4.2}_{-3.0}$	18.3 $^{+1.9}_{-1.2}$	24.6 $^{+5.1}_{-3.4}$	18.4 $^{+3.3}_{-3.6}$	-0.03 $^{+0.14}_{-0.19}$	1.55 $^{+0.40}_{-0.60}$	0.29 $^{+0.06}_{-0.10}$	41.1 $^{+3.9}_{-2.8}$	0.67 $^{+0.06}_{-0.07}$	150	15.3 $^{+0.2}_{-0.3}$
GW190412	38.4 $^{+3.8}_{-3.7}$	13.3 $^{+0.4}_{-0.3}$	30.1 $^{+4.7}_{-5.1}$	8.3 $^{+1.6}_{-0.9}$	0.25 $^{+0.08}_{-0.11}$	0.74 $^{+0.14}_{-0.17}$	0.15 $^{+0.03}_{-0.03}$	37.3 $^{+3.9}_{-3.8}$	0.67 $^{+0.05}_{-0.06}$	21	18.9 $^{+0.2}_{-0.3}$
GW190413_052954	58.6 $^{+13.3}_{-9.7}$	24.6 $^{+5.5}_{-4.1}$	34.7 $^{+12.6}_{-8.1}$	23.7 $^{+7.3}_{-6.7}$	-0.01 $^{+0.29}_{-0.34}$	3.55 $^{+2.27}_{-1.66}$	0.59 $^{+0.29}_{-0.24}$	56.0 $^{+12.5}_{-9.2}$	0.68 $^{+0.12}_{-0.13}$	1500	8.9 $^{+0.4}_{-0.7}$
GW190413_134308	78.8 $^{+17.4}_{-11.9}$	33.0 $^{+5.2}_{-4.2}$	47.5 $^{+13.5}_{-10.7}$	31.8 $^{+11.7}_{-10.8}$	-0.03 $^{+0.25}_{-0.25}$	4.45 $^{+2.48}_{-2.12}$	0.71 $^{+0.31}_{-0.30}$	75.5 $^{+16.4}_{-11.4}$	0.68 $^{+0.10}_{-0.12}$	730	10.0 $^{+0.4}_{-0.4}$
GW190421_213856	72.9 $^{+13.4}_{-9.2}$	31.2 $^{+5.9}_{-4.2}$	41.3 $^{+10.4}_{-6.9}$	31.9 $^{+8.0}_{-8.8}$	-0.06 $^{+0.22}_{-0.27}$	2.88 $^{+1.37}_{-1.38}$	0.49 $^{+0.19}_{-0.21}$	69.7 $^{+12.5}_{-8.7}$	0.67 $^{+0.10}_{-0.11}$	1200	10.7 $^{+0.2}_{-0.2}$
GW190424_180648	72.6 $^{+13.3}_{-10.7}$	31.0 $^{+5.8}_{-4.6}$	40.5 $^{+11.1}_{-7.3}$	31.8 $^{+7.6}_{-7.7}$	0.13 $^{+0.22}_{-0.22}$	2.20 $^{+1.58}_{-1.16}$	0.39 $^{+0.23}_{-0.19}$	68.9 $^{+12.4}_{-10.1}$	0.74 $^{+0.09}_{-0.09}$	28000	10.4 $^{+0.2}_{-0.4}$
GW190425	3.4 $^{+0.3}_{-0.1}$	1.44 $^{+0.02}_{-0.02}$	2.0 $^{+0.6}_{-0.3}$	1.4 $^{+0.3}_{-0.3}$	0.06 $^{+0.11}_{-0.05}$	0.16 $^{+0.07}_{-0.07}$	0.03 $^{+0.01}_{-0.02}$	-	-	10000	12.4 $^{+0.3}_{-0.4}$
GW190426_152155	7.2 $^{+3.5}_{-1.5}$	2.41 $^{+0.08}_{-0.08}$	5.7 $^{+3.9}_{-2.3}$	1.5 $^{+0.8}_{-0.5}$	-0.03 $^{+0.32}_{-0.30}$	0.37 $^{+0.18}_{-0.16}$	0.08 $^{+0.04}_{-0.03}$	-	-	1300	8.7 $^{+0.5}_{-0.6}$
GW190503_185404	71.7 $^{+9.4}_{-8.3}$	30.2 $^{+4.2}_{-4.2}$	43.3 $^{+9.2}_{-5.8}$	28.4 $^{+7.7}_{-8.0}$	-0.03 $^{+0.20}_{-0.26}$	1.45 $^{+0.69}_{-0.63}$	0.27 $^{+0.11}_{-0.11}$	68.6 $^{+8.8}_{-7.7}$	0.66 $^{+0.09}_{-0.12}$	94	12.4 $^{+0.2}_{-0.3}$
GW190512_180714	35.9 $^{+3.8}_{-3.5}$	14.6 $^{+1.3}_{-1.0}$	23.3 $^{+5.3}_{-5.8}$	12.6 $^{+3.6}_{-2.5}$	0.03 $^{+0.12}_{-0.13}$	1.43 $^{+0.55}_{-0.55}$	0.27 $^{+0.09}_{-0.10}$	34.5 $^{+3.8}_{-3.5}$	0.65 $^{+0.07}_{-0.07}$	220	12.2 $^{+0.2}_{-0.4}$
GW190513_205428	53.9 $^{+8.6}_{-5.9}$	21.6 $^{+3.8}_{-4.8}$	35.7 $^{+9.5}_{-9.2}$	18.0 $^{+7.7}_{-4.1}$	0.11 $^{+0.28}_{-0.17}$	2.06 $^{+0.88}_{-0.80}$	0.37 $^{+0.13}_{-0.13}$	51.6 $^{+8.2}_{-5.8}$	0.68 $^{+0.14}_{-0.12}$	520	12.9 $^{+0.3}_{-0.4}$
GW190514_065416	67.2 $^{+18.7}_{-10.8}$	28.5 $^{+7.9}_{-4.8}$	39.0 $^{+14.7}_{-8.2}$	28.4 $^{+9.3}_{-8.8}$	-0.19 $^{+0.29}_{-0.32}$	4.13 $^{+2.65}_{-2.17}$	0.67 $^{+0.33}_{-0.31}$	64.5 $^{+17.9}_{-10.4}$	0.63 $^{+0.11}_{-0.15}$	3000	8.2 $^{+0.3}_{-0.3}$
GW190517_055101	63.5 $^{+9.6}_{-9.6}$	26.6 $^{+4.0}_{-4.0}$	37.4 $^{+11.7}_{-7.6}$	25.3 $^{+7.0}_{-7.3}$	0.52 $^{+0.19}_{-0.19}$	1.86 $^{+1.62}_{-0.84}$	0.34 $^{+0.24}_{-0.14}$	59.3 $^{+9.1}_{-8.9}$	0.87 $^{+0.05}_{-0.07}$	470	10.7 $^{+0.4}_{-0.6}$
GW190519_153544	106.6 $^{+13.5}_{-14.8}$	44.5 $^{+6.4}_{-7.1}$	66.0 $^{+10.7}_{-12.0}$	40.5 $^{+11.0}_{-11.1}$	0.31 $^{+0.20}_{-0.22}$	2.53 $^{+1.83}_{-0.92}$	0.44 $^{+0.25}_{-0.14}$	101.0 $^{+12.4}_{-13.8}$	0.79 $^{+0.07}_{-0.13}$	860	15.6 $^{+0.2}_{-0.3}$
GW190521	163.9 $^{+39.2}_{-23.5}$	69.2 $^{+17.0}_{-10.6}$	95.3 $^{+28.7}_{-18.9}$	69.0 $^{+22.7}_{-23.1}$	0.03 $^{+0.32}_{-0.39}$	3.92 $^{+2.19}_{-1.95}$	0.64 $^{+0.28}_{-0.28}$	156.3 $^{+36.8}_{-22.4}$	0.71 $^{+0.12}_{-0.16}$	1000	14.2 $^{+0.3}_{-0.3}$
GW190521_074359	74.7 $^{+7.0}_{-4.8}$	32.1 $^{+3.2}_{-2.5}$	42.2 $^{+5.9}_{-4.8}$	32.8 $^{+5.4}_{-6.4}$	0.09 $^{+0.10}_{-0.13}$	1.24 $^{+0.40}_{-0.57}$	0.24 $^{+0.07}_{-0.10}$	71.0 $^{+6.5}_{-4.4}$	0.72 $^{+0.05}_{-0.07}$	550	25.8 $^{+0.1}_{-0.2}$
GW190527_092055	59.1 $^{+21.3}_{-9.8}$	24.3 $^{+9.1}_{-4.2}$	36.5 $^{+16.4}_{-8.1}$	22.6 $^{+10.5}_{-10.5}$	0.11 $^{+0.28}_{-0.28}$	2.49 $^{+2.48}_{-1.24}$	0.44 $^{+0.34}_{-0.20}$	56.4 $^{+20.2}_{-9.3}$	0.71 $^{+0.12}_{-0.16}$	3700	8.1 $^{+0.3}_{-0.9}$
GW190602_175927	116.3 $^{+19.0}_{-15.6}$	49.1 $^{+9.1}_{-8.5}$	69.1 $^{+15.7}_{-13.0}$	47.8 $^{+14.3}_{-17.4}$	0.07 $^{+0.25}_{-0.24}$	2.69 $^{+1.79}_{-1.12}$	0.47 $^{+0.25}_{-0.17}$	110.9 $^{+17.0}_{-14.9}$	0.70 $^{+0.10}_{-0.14}$	690	12.8 $^{+0.2}_{-0.3}$
GW190620_030421	92.1 $^{+18.5}_{-13.1}$	38.3 $^{+8.3}_{-6.5}$	57.1 $^{+16.0}_{-12.7}$	35.5 $^{+12.2}_{-12.3}$	0.33 $^{+0.22}_{-0.25}$	2.81 $^{+1.68}_{-1.31}$	0.49 $^{+0.23}_{-0.20}$	87.2 $^{+16.8}_{-12.1}$	0.79 $^{+0.08}_{-0.15}$	7200	12.1 $^{+0.3}_{-0.4}$
GW190630_185205	59.1 $^{+4.6}_{-4.8}$	24.9 $^{+2.1}_{-2.1}$	35.1 $^{+6.9}_{-5.6}$	23.7 $^{+5.2}_{-5.1}$	0.10 $^{+0.12}_{-0.13}$	0.89 $^{+0.56}_{-0.37}$	0.18 $^{+0.10}_{-0.07}$	56.4 $^{+4.4}_{-4.6}$	0.70 $^{+0.05}_{-0.07}$	1200	15.6 $^{+0.2}_{-0.3}$
GW190701_203306	94.3 $^{+12.1}_{-9.5}$	40.3 $^{+5.4}_{-4.9}$	53.9 $^{+11.8}_{-12.0}$	40.8 $^{+8.7}_{-8.7}$	-0.07 $^{+0.23}_{-0.29}$	2.06 $^{+0.76}_{-0.73}$	0.37 $^{+0.11}_{-0.12}$	90.2 $^{+11.3}_{-8.9}$	0.66 $^{+0.09}_{-0.13}$	46	11.3 $^{+0.2}_{-0.3}$
GW190706_222641	104.1 $^{+20.2}_{-13.5}$	42.7 $^{+10.0}_{-7.0}$	67.0 $^{+14.6}_{-16.2}$	38.2 $^{+14.6}_{-13.3}$	0.28 $^{+0.26}_{-0.29}$	4.42 $^{+2.59}_{-1.93}$	0.71 $^{+0.32}_{-0.27}$	99.0 $^{+18.3}_{-13.5}$	0.78 $^{+0.09}_{-0.18}$	650	12.6 $^{+0.2}_{-0.4}$
GW190707_093326	20.1 $^{+1.9}_{-1.3}$	8.5 $^{+0.6}_{-0.5}$	11.6 $^{+3.3}_{-1.7}$	8.4 $^{+1.4}_{-1.7}$	-0.05 $^{+0.10}_{-0.08}$	0.77 $^{+0.38}_{-0.37}$	0.16 $^{+0.07}_{-0.07}$	19.2 $^{+1.9}_{-1.3}$	0.66 $^{+0.03}_{-0.04}$	1300	13.3 $^{+0.2}_{-0.4}$
GW190708_232457	30.9 $^{+2.5}_{-1.8}$	13.2 $^{+0.9}_{-0.6}$	17.6 $^{+4.7}_{-2.3}$	13.2 $^{+2.0}_{-2.7}$	0.02 $^{+0.10}_{-0.08}$	0.88 $^{+0.33}_{-0.39}$	0.18 $^{+0.06}_{-0.07}$	29.5 $^{+2.5}_{-1.8}$	0.69 $^{+0.04}_{-0.04}$	14000	13.1 $^{+0.2}_{-0.3}$
GW190719_215514	57.8 $^{+18.3}_{-10.7}$	23.5 $^{+6.5}_{-4.0}$	36.5 $^{+18.0}_{-10.3}$	20.8 $^{+9.0}_{-7.2}$	0.32 $^{+0.29}_{-0.31}$	3.94 $^{+2.59}_{-2.00}$	0.64 $^{+0.33}_{-0.29}$	54.9 $^{+17.3}_{-10.2}$	0.78 $^{+0.11}_{-0.17}$	2900	8.3 $^{+0.3}_{-0.8}$
GW190720_000836	21.5 $^{+4.3}_{-2.3}$	8.9 $^{+0.8}_{-0.8}$	13.4 $^{+6.7}_{-3.0}$	7.8 $^{+2.3}_{-2.2}$	0.18 $^{+0.14}_{-0.12}$	0.79 $^{+0.69}_{-0.32}$	0.16 $^{+0.12}_{-0.06}$	20.4 $^{+4.5}_{-2.2}$	0.72 $^{+0.06}_{-0.05}$	460	11.0 $^{+0.3}_{-0.7}$
GW190727_060333	67.1 $^{+11.7}_{-8.0}$	28.6 $^{+5.3}_{-3.7}$	38.0 $^{+9.5}_{-6.2}$	29.4 $^{+7.1}_{-8.4}$	0.11 $^{+0.26}_{-0.25}$	3.30 $^{+1.54}_{-1.50}$	0.55 $^{+0.21}_{-0.22}$	63.8 $^{+10.9}_{-7.5}$	0.73 $^{+0.10}_{-0.10}$	830	11.9 $^{+0.3}_{-0.5}$
GW190728_064510	20.6 $^{+4.5}_{-1.3}$	8.0 $^{+0.5}_{-0.3}$	12.3 $^{+7.2}_{-2.2}$	8.1 $^{+1.7}_{-2.6}$	0.12 $^{+0.20}_{-0.07}$	0.87 $^{+0.26}_{-0.37}$	0.18 $^{+0.05}_{-0.05}$	19.6 $^{+4.7}_{-1.3}$	0.71 $^{+0.04}_{-0.04}$	400	13.0 $^{+0.2}_{-0.4}$
GW190731_140936	70.1 $^{+15.8}_{-11.3}$	29.5 $^{+7.1}_{-5.2}$	41.5 $^{+12.2}_{-9.0}$	28.8 $^{+9.7}_{-9.5}$	0.06 $^{+0.24}_{-0.24}$	3.30 $^{+2.39}_{-1.72}$	0.55 $^{+0.31}_{-0.26}$	67.0 $^{+14.6}_{-10.8}$	0.70 $^{+0.10}_{-0.13}$	3400	8.7 $^{+0.2}_{-0.5}$
GW190803_022701	64.5 $^{+12.6}_{-9.0}$	27.3 $^{+5.7}_{-4.1}$	37.3 $^{+10.6}_{-7.0}$	27.3 $^{+7.8}_{-8.2}$	-0.03 $^{+0.24}_{-0.27}$	3.27 $^{+1.95}_{-1.58}$	0.55 $^{+0.26}_{-0.24}$	61.7 $^{+11.8}_{-8.5}$	0.68 $^{+0.10}_{-0.11}$	1500	8.6 $^{+0.3}_{-0.5}$
GW190814	25.8 $^{+1.0}_{-0.9}$	6.09 $^{+0.06}_{-0.06}$	23.2 $^{+1.1}_{-1.0}$	2.59 $^{+0.08}_{-0.09}$	0.00 $^{+0.06}_{-0.06}$	0.24 $^{+0.04}_{-0.05}$	0.05 $^{+0.009}_{-0.010}$	25.6 $^{+1.1}_{-0.9}$	0.28 $^{+0.02}_{-0.02}$	19	24.9 $^{+0.1}_{-0.2}$
GW190828_063405	58.0 $^{+7.7}_{-4.8}$	25.0 $^{+3.4}_{-2.1}$	32.1 $^{+5.8}_{-4.0}$	26.2 $^{+4.6}_{-4.8}$	0.19 $^{+0.15}_{-0.16}$	2.13 $^{+0.66}_{-0.93}$	0.38 $^{+0.10}_{-0.15}$	54.9 $^{+7.2}_{-4.3}$	0.75 $^{+0.06}_{-0.07}$	520	16.2 $^{+0.2}_{-0.3}$
GW190828_065509	34.4 $^{+5.4}_{-4.4}$	13.3 $^{+1.2}_{-1.0}$	24.1 $^{+7.0}_{-7.2}$	10.2 $^{+3.6}_{-2.1}$	0.08 $^{+0.16}_{-0.16}$	1.60 $^{+0.62}_{-0.60}$	0.30 $^{+0.10}_{-0.10}$	33.1 $^{+5.5}_{-4.5}$	0.65 $^{+0.08}_{-0.08}$	660	10.0 $^{+0.3}_{-0.5}$
GW190909_114149	75.0 $^{+55.9}_{-17.6}$	30.9 $^{+7.2}_{-15.2}$	45.8 $^{+52.7}_{-13.3}$	28.3 $^{+13.4}_{-10.6}$	-0.06 $^{+0.37}_{-0.36}$	3.77 $^{+3.27}_{-2.22}$	0.62 $^{+0.41}_{-0.33}$	72.0 $^{+54.9}_{-16.8}$	0.66 $^{+0.15}_{-0.20}$	4700	8.1 $^{+0.4}_{-0.6}$
GW190910_112807	79.6 $^{+9.3}_{-9.1}$	34.3 $^{+4.1}_{-4.1}$	43.9 $^{+7.6}_{-6.1}$	35.6 $^{+6.3}_{-7.2}$	0.02 $^{+0.18}_{-0.18}$	1.46 $^{+1.03}_{-0.58}$	0.28 $^{+0.16}_{-0.10}$	75.8 $^{+8.5}_{-8.6}$	0.70 $^{+0.08}_{-0.07}$	11000	14.1 $^{+0.2}_{-0.3}$
GW190915_235702	59.9 $^{+7.5}_{-6.4}$	25.3 $^{+3.2}_{-2.7}$	35.3 $^{+9.5}_{-6.4}$	24.4 $^{+5.6}_{-6.1}$	0.02 $^{+0.20}_{-0.25}$	1.62 $^{+0.71}_{-0.61}$	0.30 $^{+0.11}_{-0.10}$	57.2 $^{+7.1}_{-6.0}$	0.70 $^{+0.09}_{-0.11}$	400	13.6 $^{+0.2}_{-0.3}$
GW190924_021846	13.9 $^{+5.1}_{-1.0}$	5.8 $^{+0.2}_{-0.2}$	8.9 $^{+7.0}_{-2.0}$	5.0 $^{+1.4}_{-1.9}$	0.03 $^{+0.30}_{-0.09}$	0.57 $^{+0.22}_{-0.22}$	0.12 $^{+0.04}_{-0.04}$	13.3 $^{+5.2}_{-1.0}$	0.67 $^{+0.05}_{-0.05}$	360	11.5 $^{+0.3}_{-0.4}$
GW190929_012149	104.3 $^{+34.9}_{-25.2}$	35.8 $^{+14.9}_{-8.2}$	80.8 $^{+33.0}_{-33.2}$	24.1 $^{+19.3}_{-10.6}$	0.01 $^{+0.34}_{-0.33}$	2.13 $^{+3.65}_{-1.05}$	0.38 $^{+0.49}_{-0.17}$	101.5 $^{+33.6}_{-25.3}$	0.66 $^{+0.20}_{-0.31}$	2200	10.1 $^{+0.6}_{-0.8}$
GW190930_133541	20.3 $^{+8.9}_{-1.5}$	8.5 $^{+0.5}_{-0.5}$	12.3 $^{+12.4}_{-2.3}$	7.8 $^{+1.7}_{-3.3}$	0.14 $^{+0.31}_{-0.15}$	0.76 $^{+0.36}_{-0.32}$	0.15 $^{+0.06}_{-0.06}$	19.4 $^{+9.2}_{-1.5}$	0.72 $^{+0.07}_{-0.06}$	1700	9.5 $^{+0.3}_{-0.5}$

O3 Public Alerts by Month



O3a (Apr – Sep 2019)

39 events, 3 with $M < 3 M_{\text{SUN}}$:

GW 190425 -> BNS, 10^4 deg 2 skymap

GW 190426 -> BHNS, 10^3 deg 2 skymap

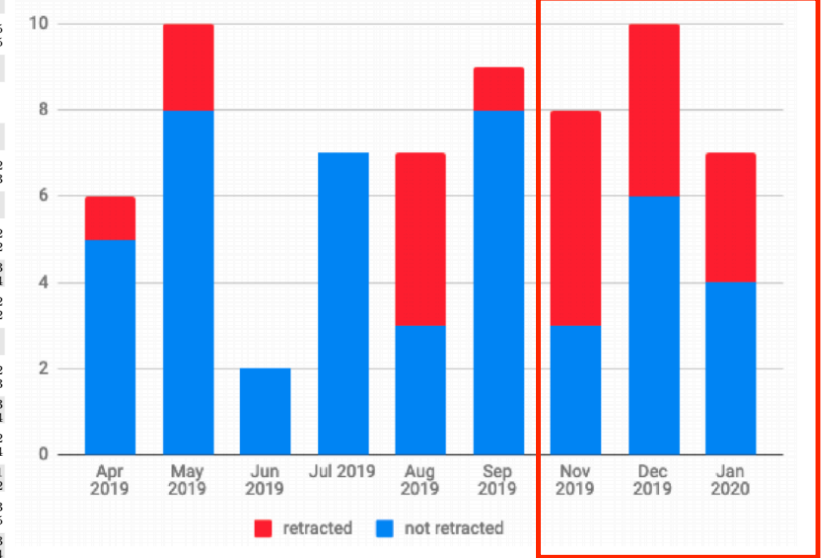
GW190814 -> (?) BHNS, 19 deg 2 skymap

The GW era – O3b



Event	M (M_{\odot})	\mathcal{M} (M_{\odot})	m_1 (M_{\odot})	m_2 (M_{\odot})	χ_{eff}	D_L (Gpc)	z	M_f (M_{\odot})	χ_f	$\Delta\Omega$ (deg ²)	SNR
GW191103.012549	20.0 ^{+3.7} _{-1.8}	8.34 ^{+0.66} _{-0.57}	11.8 ^{+6.2} _{-2.2}	7.9 ^{+1.7} _{-2.4}	0.21 ^{+0.16} _{-0.10}	0.99 ^{+0.50} _{-0.47}	0.20 ^{+0.09} _{-0.09}	19.0 ^{+3.8} _{-1.7}	0.75 ^{+0.06} _{-0.05}	2500	8.9 ^{+0.3} _{-0.5}
GW191105.143521	18.5 ^{+2.1} _{-1.3}	7.82 ^{+0.61} _{-0.45}	10.7 ^{+3.7} _{-1.6}	7.7 ^{+1.4} _{-1.9}	-0.02 ^{+0.13} _{-0.09}	1.15 ^{+0.43} _{-0.48}	0.23 ^{+0.07} _{-0.09}	17.6 ^{+2.1} _{-1.2}	0.67 ^{+0.04} _{-0.05}	640	9.7 ^{+0.3} _{-0.5}
GW191109.010717	112 ⁺²⁰ ₋₁₆	47.5 ^{+9.6} _{-7.5}	65 ⁺¹¹ ₋₁₁	47 ⁺¹⁵ ₋₁₃	-0.29 ^{+0.42} _{-0.31}	1.29 ^{+1.13} _{-0.65}	0.25 ^{+0.18} _{-0.12}	107 ⁺¹⁸ ₋₁₅	0.61 ^{+0.18} _{-0.19}	1600	17.3 ^{+0.5} _{-1.1}
GW191113.071753	34.5 ^{+10.5} _{-9.8}	10.7 ^{+1.1} _{-1.0}	29 ⁺¹² ₋₁₄	5.9 ^{+4.4} _{-1.3}	0.00 ^{+0.37} _{-0.29}	1.37 ^{+1.15} _{-0.62}	0.26 ^{+0.18} _{-0.11}	34 ⁺¹¹ ₋₁₀	0.45 ^{+0.33} _{-0.11}	3600	7.9 ^{+0.5} _{-1.2}
GW191126.115259	20.7 ^{+3.4} _{-2.0}	8.65 ^{+0.95} _{-0.71}	12.1 ^{+5.5} _{-2.2}	8.3 ^{+1.9} _{-2.4}	0.21 ^{+0.15} _{-0.11}	1.62 ^{+0.74} _{-0.74}	0.30 ^{+0.12} _{-0.13}	19.6 ^{+3.5} _{-2.0}	0.75 ^{+0.06} _{-0.05}	1400	8.3 ^{+0.2} _{-0.5}
GW191127.050227	80 ⁺³⁹ ₋₂₂	29.9 ^{+11.7} _{-9.1}	53 ⁺⁴⁷ ₋₂₀	24 ⁺¹⁷ ₋₁₄	0.18 ^{+0.34} _{-0.36}	3.4 ^{+3.1} _{-1.9}	0.57 ^{+0.40} _{-0.29}	76 ⁺³⁹ ₋₂₁	0.75 ^{+0.13} _{-0.29}	980	9.2 ^{+0.7} _{-0.6}
GW191129.134029	17.5 ^{+2.4} _{-1.2}	7.31 ^{+0.43} _{-0.28}	10.7 ^{+4.1} _{-2.1}	6.7 ^{+1.5} _{-1.7}	0.06 ^{+0.16} _{-0.08}	0.79 ^{+0.26} _{-0.33}	0.16 ^{+0.05} _{-0.06}	16.8 ^{+2.5} _{-1.2}	0.69 ^{+0.03} _{-0.05}	850	13.1 ^{+0.2} _{-0.3}
GW191204.110529	47.2 ^{+9.2} _{-8.0}	19.8 ^{+3.6} _{-3.3}	27.3 ^{+11.0} _{-6.0}	19.3 ^{+5.6} _{-6.0}	0.05 ^{+0.26} _{-0.27}	1.8 ^{+1.7} _{-1.1}	0.34 ^{+0.25} _{-0.18}	45.0 ^{+8.6} _{-7.6}	0.71 ^{+0.12} _{-0.11}	3700	8.8 ^{+0.4} _{-0.6}
GW191204.171526	20.21 ^{+1.70} _{-0.96}	8.55 ^{+0.38} _{-0.27}	11.9 ^{+3.3} _{-1.8}	8.2 ^{+1.4} _{-1.6}	0.16 ^{+0.08} _{-0.05}	0.65 ^{+0.19} _{-0.15}	0.13 ^{+0.04} _{-0.04}	19.21 ^{+1.79} _{-0.95}	0.73 ^{+0.03} _{-0.03}	350	17.5 ^{+0.2} _{-0.2}
GW191215.223052	43.3 ^{+5.3} _{-4.3}	18.4 ^{+2.2} _{-1.7}	24.9 ^{+7.1} _{-4.1}	18.1 ^{+3.8} _{-4.1}	-0.04 ^{+0.17} _{-0.21}	1.93 ^{+0.89} _{-0.86}	0.35 ^{+0.13} _{-0.14}	41.4 ^{+5.1} _{-4.1}	0.68 ^{+0.07} _{-0.07}	530	11.2 ^{+0.3} _{-0.4}
GW191216.213338	19.81 ^{+2.69} _{-0.94}	8.33 ^{+0.22} _{-0.19}	12.1 ^{+4.6} _{-2.3}	7.7 ^{+1.6} _{-1.9}	0.11 ^{+0.13} _{-0.06}	0.34 ^{+0.12} _{-0.13}	0.07 ^{+0.02} _{-0.03}	18.87 ^{+2.80} _{-0.94}	0.70 ^{+0.03} _{-0.04}	490	18.6 ^{+0.2} _{-0.2}
GW191219.163120	32.3 ^{+2.2} _{-2.7}	4.32 ^{+0.12} _{-0.17}	31.1 ^{+2.2} _{-2.8}	1.17 ^{+0.07} _{-0.06}	0.00 ^{+0.07} _{-0.09}	0.55 ^{+0.25} _{-0.16}	0.11 ^{+0.05} _{-0.03}	32.2 ^{+2.2} _{-2.7}	0.14 ^{+0.06} _{-0.06}	1500	9.1 ^{+0.5} _{-0.8}
GW191222.033537	79 ⁺¹⁶ ₋₁₁	33.8 ^{+7.1} _{-5.0}	45.1 ^{+10.9} _{-8.0}	34.7 ^{+9.3} _{-10.5}	-0.04 ^{+0.20} _{-0.25}	3.0 ^{+1.7} _{-1.7}	0.51 ^{+0.23} _{-0.26}	75.5 ^{+15.3} _{-9.9}	0.67 ^{+0.08} _{-0.11}	2000	12.5 ^{+0.2} _{-0.3}
GW191230.180458	86 ⁺¹⁹ ₋₁₂	36.5 ^{+8.2} _{-5.6}	49.4 ^{+14.0} _{-9.6}	37 ⁺¹¹ ₋₁₂	-0.05 ^{+0.26} _{-0.31}	4.3 ^{+2.1} _{-1.9}	0.69 ^{+0.26} _{-0.27}	82 ⁺¹⁷ ₋₁₁	0.68 ^{+0.11} _{-0.13}	1100	10.4 ^{+0.3} _{-0.4}
GW200105.162426	11.0 ^{+1.5} _{-1.4}	3.42 ^{+0.08} _{-0.08}	9.0 ^{+1.7} _{-1.7}	1.91 ^{+0.33} _{-0.24}	0.00 ^{+0.13} _{-0.18}	0.27 ^{+0.12} _{-0.11}	0.06 ^{+0.02} _{-0.02}	10.7 ^{+1.5} _{-1.4}	0.43 ^{+0.05} _{-0.02}	7900	13.7 ^{+0.2} _{-0.4}
GW200112.155838	63.9 ^{+5.7} _{-4.6}	27.4 ^{+2.6} _{-2.1}	35.6 ^{+6.7} _{-4.5}	28.3 ^{+4.4} _{-5.9}	0.06 ^{+0.15} _{-0.15}	1.25 ^{+0.43} _{-0.46}	0.24 ^{+0.07} _{-0.08}	60.8 ^{+5.3} _{-4.3}	0.71 ^{+0.06} _{-0.06}	4300	19.8 ^{+0.1} _{-0.2}
GW200115.042309	7.4 ^{+1.8} _{-1.7}	2.43 ^{+0.05} _{-0.07}	5.9 ^{+2.0} _{-2.5}	1.44 ^{+0.85} _{-0.29}	-0.15 ^{+0.24} _{-0.42}	0.29 ^{+0.15} _{-0.10}	0.06 ^{+0.03} _{-0.02}	7.2 ^{+1.8} _{-1.7}	0.42 ^{+0.09} _{-0.05}	370	11.3 ^{+0.3} _{-0.5}
GW200128.022011	75 ⁺¹⁷ ₋₁₂	32.0 ^{+7.5} _{-5.5}	42.2 ^{+11.6} _{-8.1}	32.6 ^{+9.5} _{-9.2}	0.12 ^{+0.24} _{-0.25}	3.4 ^{+2.1} _{-1.8}	0.56 ^{+0.28} _{-0.28}	71 ⁺¹⁶ ₋₁₁	0.74 ^{+0.10} _{-0.10}	2600	10.6 ^{+0.3} _{-0.4}
GW200129.065458	63.4 ^{+4.3} _{-3.6}	27.2 ^{+2.1} _{-2.3}	34.5 ^{+9.9} _{-3.2}	28.9 ^{+3.4} _{-9.3}	0.11 ^{+0.11} _{-0.16}	0.90 ^{+0.29} _{-0.38}	0.18 ^{+0.05} _{-0.07}	60.3 ^{+4.0} _{-3.3}	0.73 ^{+0.06} _{-0.05}	130	26.8 ^{+0.2} _{-0.2}
GW200202.154313	17.58 ^{+1.78} _{-0.67}	7.49 ^{+0.24} _{-0.20}	10.1 ^{+3.5} _{-1.4}	7.3 ^{+1.7} _{-1.7}	0.04 ^{+0.13} _{-0.06}	0.41 ^{+0.15} _{-0.16}	0.09 ^{+0.03} _{-0.03}	16.76 ^{+1.87} _{-0.66}	0.69 ^{+0.03} _{-0.04}	170	10.8 ^{+0.2} _{-0.4}
GW200208.130117	65.4 ^{+7.8} _{-6.8}	27.7 ^{+3.6} _{-3.1}	37.8 ^{+9.2} _{-6.2}	27.4 ^{+6.1} _{-7.4}	-0.07 ^{+0.22} _{-0.27}	2.23 ^{+1.00} _{-0.85}	0.40 ^{+0.15} _{-0.14}	62.5 ^{+7.3} _{-6.4}	0.66 ^{+0.09} _{-0.13}	30	10.8 ^{+0.3} _{-0.4}
GW200208.222617	63 ⁺¹⁰⁰ ₋₂₅	19.6 ^{+10.7} _{-5.1}	51 ⁺¹⁰⁴ ₋₃₀	12.3 ^{+9.0} _{-5.7}	0.45 ^{+0.43} _{-0.44}	4.1 ^{+4.4} _{-1.9}	0.66 ^{+0.54} _{-0.28}	61 ⁺¹⁰⁰ ₋₂₅	0.83 ^{+0.14} _{-0.27}	2000	7.4 ^{+1.4} _{-1.2}
GW200209.085452	62.6 ^{+13.9} _{-9.4}	26.7 ^{+6.0} _{-4.2}	35.6 ^{+10.5} _{-6.8}	27.1 ^{+7.8} _{-7.8}	-0.12 ^{+0.24} _{-0.30}	3.4 ^{+1.9} _{-1.8}	0.57 ^{+0.25} _{-0.26}	59.9 ^{+13.1} _{-8.9}	0.66 ^{+0.10} _{-0.12}	730	9.6 ^{+0.4} _{-0.5}
GW200210.092254	27.0 ^{+7.1} _{-4.3}	6.56 ^{+0.38} _{-0.40}	24.1 ^{+7.5} _{-4.6}	2.83 ^{+0.47} _{-0.42}	0.02 ^{+0.22} _{-0.21}	0.94 ^{+0.43} _{-0.34}	0.19 ^{+0.08} _{-0.06}	26.7 ^{+7.2} _{-4.3}	0.34 ^{+0.13} _{-0.08}	1800	8.4 ^{+0.5} _{-0.7}
GW200216.220804	81 ⁺²⁰ ₋₁₄	32.9 ^{+9.3} _{-8.5}	51 ⁺²² ₋₁₃	30 ⁺¹⁴ ₋₁₆	0.10 ^{+0.34} _{-0.36}	3.8 ^{+3.0} _{-2.0}	0.63 ^{+0.37} _{-0.29}	78 ⁺¹⁹ ₋₁₃	0.70 ^{+0.14} _{-0.24}	2900	8.1 ^{+0.4} _{-0.5}
GW200219.094415	65.0 ^{+12.6} _{-8.2}	27.6 ^{+5.6} _{-3.8}	37.5 ^{+10.1} _{-6.9}	27.9 ^{+7.4} _{-8.4}	-0.08 ^{+0.23} _{-0.29}	3.4 ^{+1.7} _{-1.5}	0.57 ^{+0.22} _{-0.22}	62.2 ^{+11.7} _{-7.8}	0.66 ^{+0.10} _{-0.13}	700	10.7 ^{+0.3} _{-0.5}
GW200220.061928	148 ⁺⁵⁵ ₋₃₃	62 ⁺²³ ₋₁₅	87 ⁺⁴⁰ ₋₂₃	61 ⁺²⁶ ₋₂₅	0.06 ^{+0.40} _{-0.38}	6.0 ^{+4.8} _{-3.1}	0.90 ^{+0.55} _{-0.40}	141 ⁺⁵¹ ₋₃₁	0.71 ^{+0.15} _{-0.17}	3000	7.2 ^{+0.4} _{-0.7}
GW200220.124850	67 ⁺¹⁷ ₋₁₂	28.2 ^{+7.3} _{-5.1}	38.9 ^{+14.1} _{-8.6}	27.9 ^{+9.2} _{-9.0}	-0.07 ^{+0.27} _{-0.33}	4.0 ^{+2.8} _{-2.2}	0.66 ^{+0.36} _{-0.31}	64 ⁺¹⁶ ₋₁₁	0.67 ^{+0.11} _{-0.14}	3200	8.5 ^{+0.3} _{-0.5}
GW200224.222234	72.2 ^{+7.2} _{-5.1}	31.1 ^{+3.2} _{-2.6}	40.0 ^{+6.9} _{-4.5}	32.5 ^{+5.0} _{-7.2}	0.10 ^{+0.15} _{-0.15}	1.71 ^{+0.49} _{-0.64}	0.32 ^{+0.08} _{-0.11}	68.6 ^{+6.6} _{-4.7}	0.73 ^{+0.07} _{-0.07}	50	20.0 ^{+0.2} _{-0.2}
GW200225.060421	33.5 ^{+3.6} _{-3.0}	14.2 ^{+1.5} _{-1.4}	19.3 ^{+5.0} _{-3.0}	14.0 ^{+2.8} _{-3.5}	-0.12 ^{+0.17} _{-0.28}	1.15 ^{+0.51} _{-0.53}	0.22 ^{+0.09} _{-0.10}	32.1 ^{+3.5} _{-2.8}	0.66 ^{+0.07} _{-0.13}	370	12.5 ^{+0.3} _{-0.4}
GW200302.015811	57.8 ^{+9.6} _{-6.9}	23.4 ^{+4.7} _{-3.0}	37.8 ^{+8.7} _{-8.5}	20.0 ^{+8.1} _{-5.7}	0.01 ^{+0.25} _{-0.26}	1.48 ^{+1.02} _{-0.70}	0.28 ^{+0.16} _{-0.12}	55.5 ^{+8.9} _{-6.6}	0.66 ^{+0.13} _{-0.15}	6000	10.8 ^{+0.3} _{-0.4}
GW200306.093714	43.9 ^{+11.8} _{-7.5}	17.5 ^{+3.5} _{-3.0}	28.3 ^{+17.1} _{-7.7}	14.8 ^{+6.5} _{-6.4}	0.32 ^{+0.28} _{-0.46}	2.1 ^{+1.7} _{-1.1}	0.38 ^{+0.24} _{-0.18}	41.7 ^{+12.3} _{-6.9}	0.78 ^{+0.11} _{-0.26}	4600	7.8 ^{+0.4} _{-0.6}
GW200308.173609*	50.6 ^{+10.9} _{-8.5}	19.0 ^{+4.8} _{-2.8}	36.4 ^{+11.2} _{-9.6}	13.8 ^{+7.2} _{-3.3}	0.65 ^{+0.16} _{-0.21}	5.4 ^{+2.7} _{-2.6}	0.83 ^{+0.32} _{-0.35}	47.4 ^{+11.1} _{-7.7}	0.91 ^{+0.03} _{-0.08}	2000	7.1 ^{+0.5} _{-0.5}
GW200311.115853	61.9 ^{+5.3} _{-4.2}	26.6 ^{+2.4} _{-2.0}	34.2 ^{+6.4} _{-3.8}	27.7 ^{+4.1} _{-5.9}	-0.02 ^{+0.16} _{-0.20}	1.17 ^{+0.28} _{-0.40}	0.23 ^{+0.05} _{-0.07}	59.0 ^{+4.8} _{-3.9}	0.69 ^{+0.07} _{-0.08}	35	17.8 ^{+0.2} _{-0.7}
GW200316.215756	21.2 ^{+7.2} _{-2.0}	8.75 ^{+0.62} _{-0.55}	13.1 ^{+10.2} _{-2.9}	7.8 ^{+1.9} _{-2.9}	0.13 ^{+0.27} _{-0.10}	1.12 ^{+0.47} _{-0.44}	0.22 ^{+0.08} _{-0.08}	20.2 ^{+7.4} _{-1.9}	0.70 ^{+0.04} _{-0.04}	190	10.3 ^{+0.4} _{-0.7}
GW200322.091133*	55 ⁺³⁷ ₋₂₇	15.5 ^{+15.7} _{-3.7}	34 ⁺⁴⁸ ₋₁₈	14.0 ^{+16.8} _{-8.7}	0.24 ^{+0.45} _{-0.51}	3.6 ^{+7.0} _{-2.0}	0.60 ^{+0.84} _{-0.30}	53 ⁺³⁸ ₋₂₆	0.78 ^{+0.16} _{-0.17}	6500	6.0 ^{+1.7} _{-1.2}

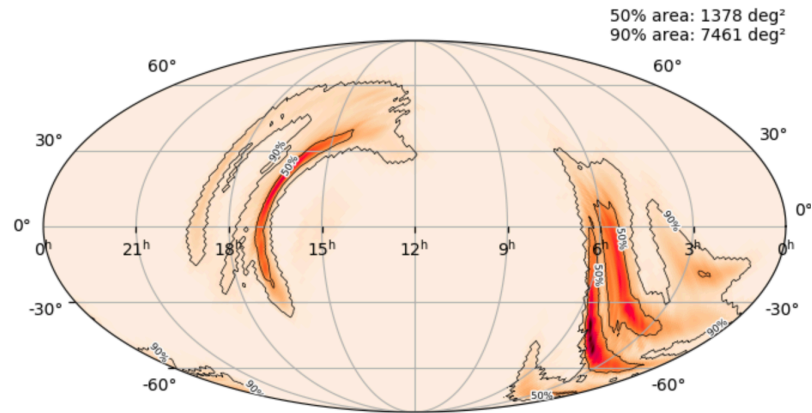
Public Alerts by Month



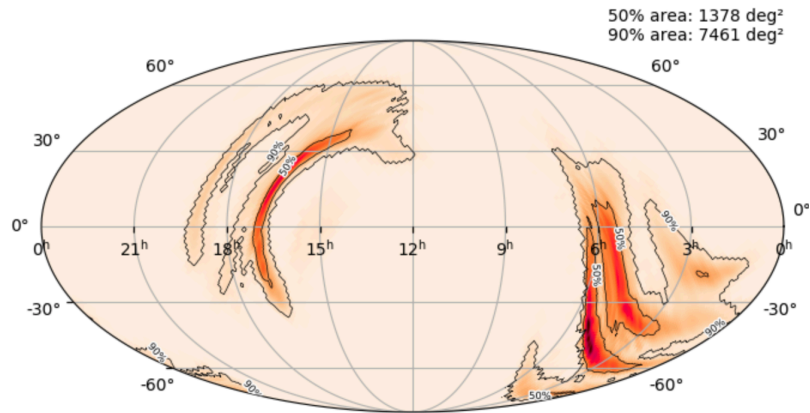
O3b (Nov 2019 – Mar 2020)
35 events, 2 with $M < 3 M_{\text{SUN}}$:

GW 191219 -> BHNS, 10^3 deg^2 skymap
GW 200210 -> BHNS/BBH, 10^3 deg^2 skymap

O3: lessons learned



O3: lessons learned



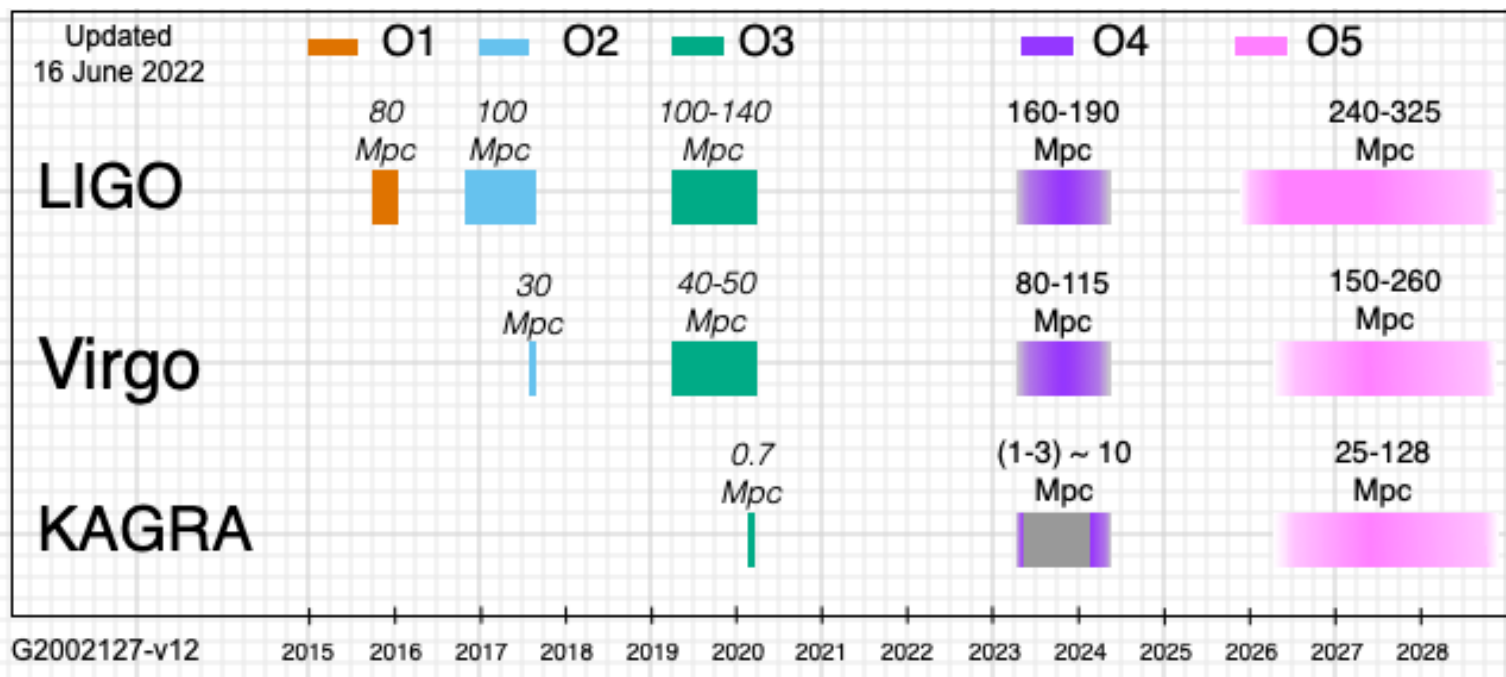
NA BEATA M !!!



O4 timeline

<https://observing.docs.ligo.org/plan/>

LIGO, Virgo, and KAGRA continue to work to prepare the detectors for the start of O4. Our ability to start O4 in March 2023 is currently under review. Unanticipated delays in some construction elements of LIGO has delayed remaining detector commissioning (...) we expect to be able to make a more confident plan for starting early in January.



During O4, we expect that four facilities (LIGO Hanford (LHO) and Livingston (LLO), KAGRA and Virgo) will observe for one year with a month break in the middle. KAGRA is expected to start with Virgo and LIGO, and then step away for commissioning and return to observing with a greater sensitivity toward the end of the O4 run.

Rates in O4 are highly uncertain: we may have > 3 GW trigger per week

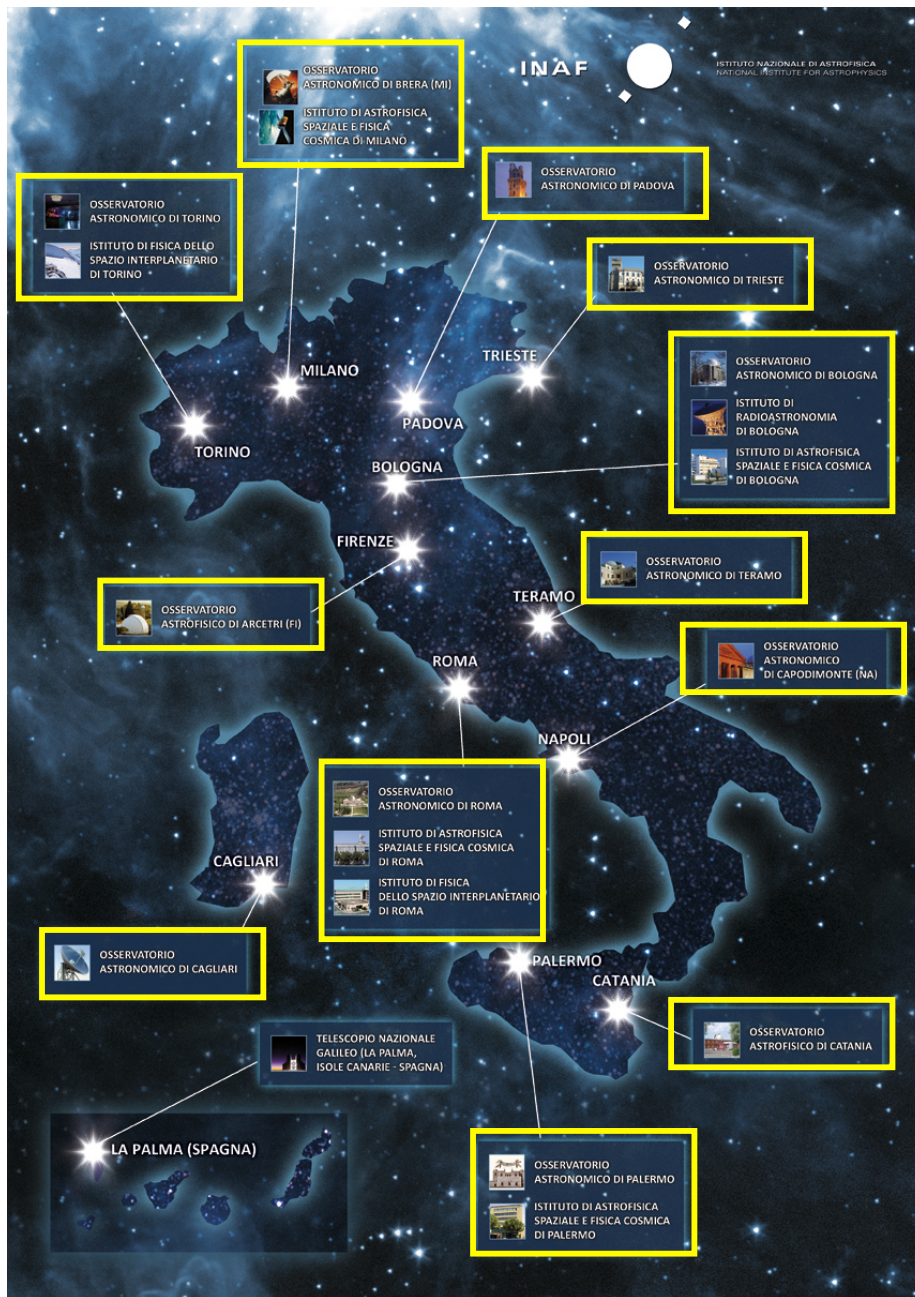
Multi-Messenger Astrophysics (GW) @ RSN4



INAF
ISTITUTO NAZIONALE
DI ASTROFISICA



Multi-Messenger Astrophysics (GW) @ RSN4



Scheda	Coordinator	# INAF Institutes	# INAF people
AGILE	C. Pittori	8	35
ET	<i>M. Branchesi</i>	13	55
Fermi Science	P. Caraveo	4	12
GAME	L. Piro	4	13
GRAWITA	E. Brocato	11	66
GRB@Mi	G. Ghirlanda	3	13
GRB@OAS	E. Pian	4	11
GuRu	S. Piranomonte	6	9
HERMES	F. Fiore	8	30
INTEGRAL	L. Natalucci	3	14
INTEGRAL HEASS	A. Malizia	3	14
LGWA	<i>J. Harms</i>	9	27
NuMerJet	R. Ciolfi	9	18
Progress	L. A. Antonelli	15	244
Swift	G. Tagliaferri	4	24

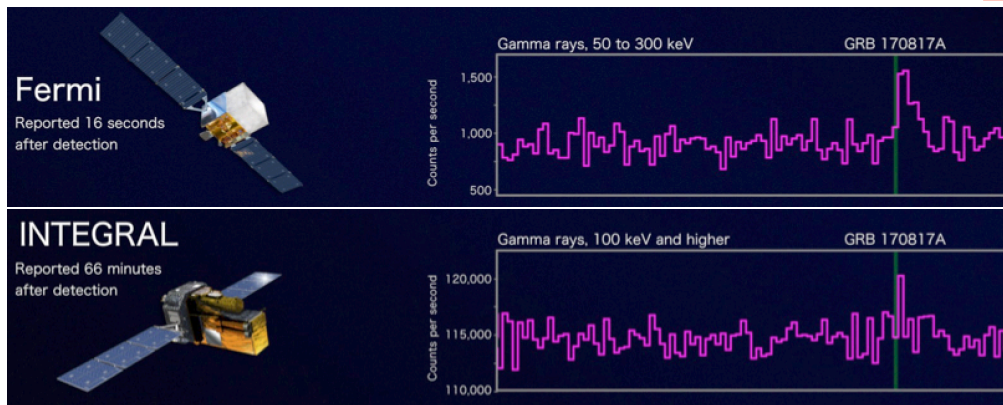
Multi-Messenger Astrophysics (GW) @ RSN4

**Search for coincident GW-GRBs
since O1**

Scheda	Coordinator	# INAF Institutes	# INAF people
AGILE	C. Pittori	8	35
ET	<i>M. Branchesi</i>	13	55
Fermi Science	P. Caraveo	4	12
GAME	L. Piro	4	13
GRAWITA	E. Brocato	11	66
GRB@Mi	G. Ghirlanda	3	13
GRB@OAS	E. Pian	4	11
GuRu	S. Piranomonte	6	9
HERMES	F. Fiore	8	30
INTEGRAL	L. Natalucci	3	14
INTEGRAL HEASS	A. Malizia	3	14
LGWA	<i>J. Harms</i>	9	27
NuMerJet	R. Ciolfi	9	18
Progress	L. A. Antonelli	15	244
Swift	G. Tagliaferri	4	24

Multi-Messenger Astrophysics (GW) @ RSN4

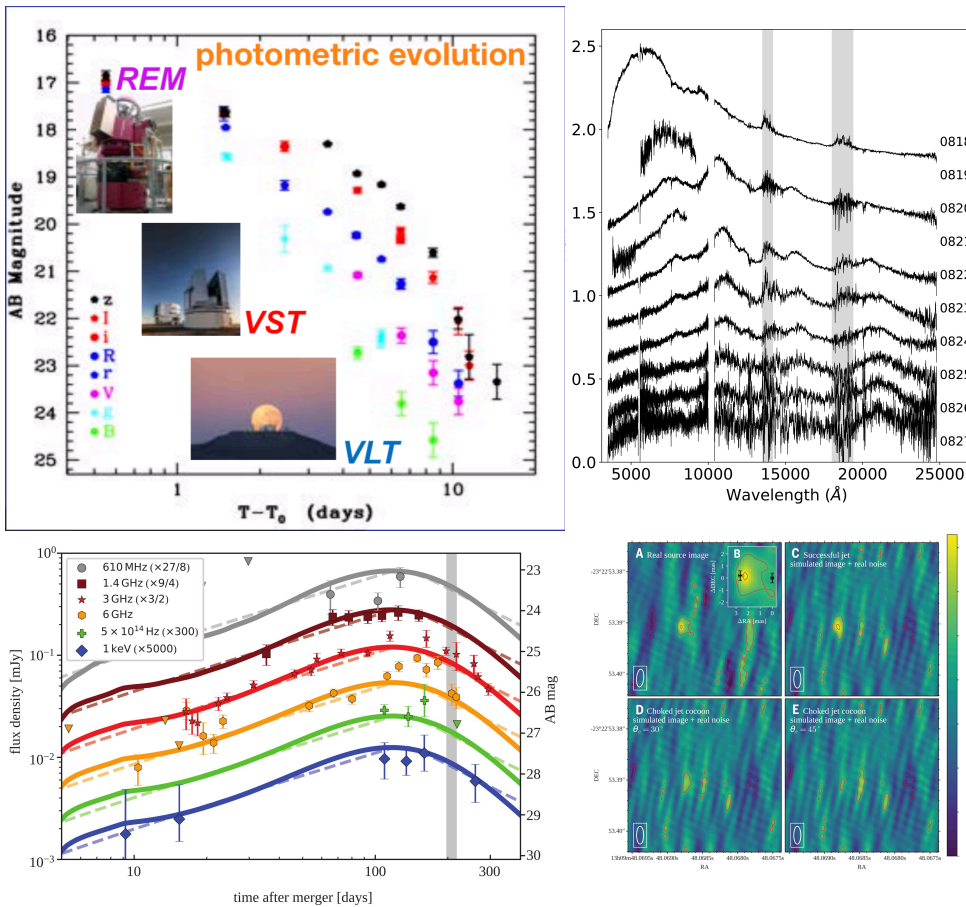
Detection of the short GRB 170817A,
associated to GW 170817



Scheda	Coordinator	# INAF Institutes	# INAF people
AGILE	C. Pittori	8	35
ET	<i>M. Branchesi</i>	13	55
Fermi Science	P. Caraveo	4	12
GAME	L. Piro	4	13
GRAWITA	E. Brocato	11	66
GRB@Mi	G. Ghirlanda	3	13
GRB@OAS	E. Pian	4	11
GuRu	S. Piranomonte	6	9
HERMES	F. Fiore	8	30
INTEGRAL	L. Natalucci	3	14
INTEGRAL HEASS	A. Malizia	3	14
LGWA	<i>J. Harms</i>	9	27
NuMerJet	R. Ciolfi	9	18
Progress	L. A. Antonelli	15	244
Swift	G. Tagliaferri	4	24

Multi-Messenger Astrophysics (GW) @ RSN4

Full characterisation of the GW 170817 KN

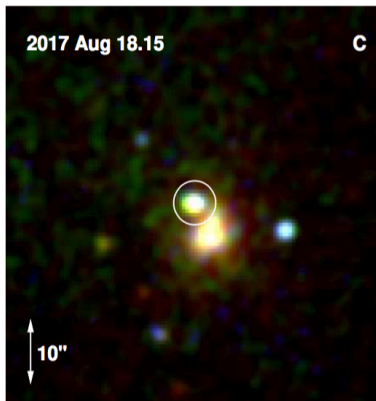


Study of the off-axis GRB afterglow emission
-> evidence for structured jet

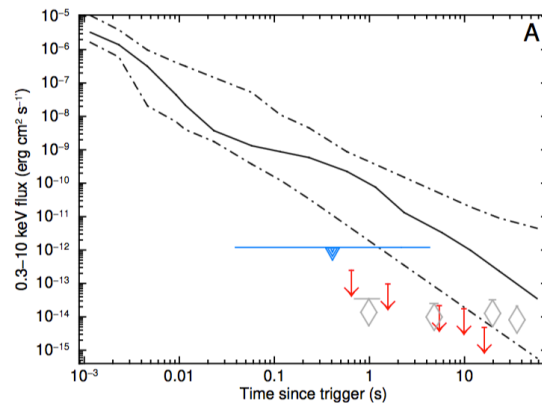
Scheda	Coordinator	# INAF Institutes	# INAF people
AGILE	C. Pittori	8	35
ET	<i>M. Branchesi</i>	13	55
Fermi Science	P. Caraveo	4	12
GAME	L. Piro	4	13
GRAWITA	E. Brocato	11	66
GRB@Mi	G. Ghirlanda	3	13
GRB@OAS	E. Pian	4	11
GuRu	S. Piranomonte	6	9
HERMES	F. Fiore	8	30
INTEGRAL	L. Natalucci	3	14
INTEGRAL HEASS	A. Malizia	3	14
LGWA	<i>J. Harms</i>	9	27
NuMerJet	R. Ciolfi	9	18
Progress	L. A. Antonelli	15	244
Swift	G. Tagliaferri	4	24

Multi-Messenger Astrophysics (GW) @ RSN4

1st (unique) UV
KN detection
(blue KN)



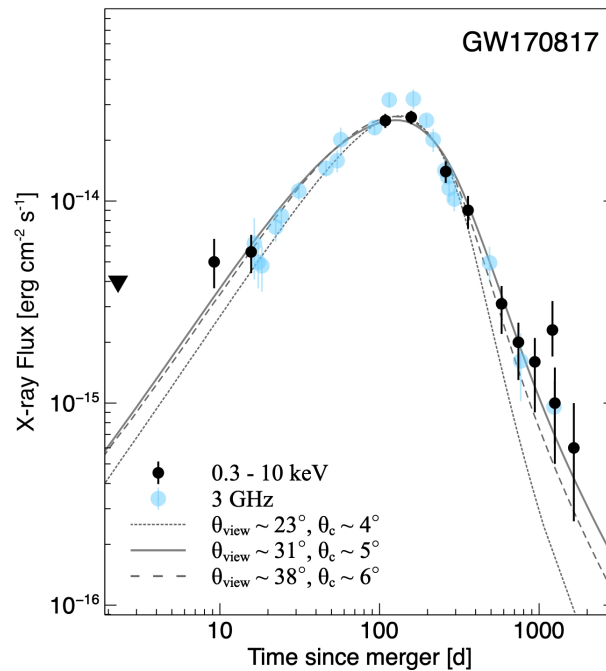
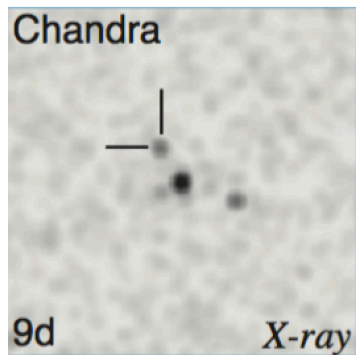
Early-time X-ray limits
(1st hint for GRB off-
axis emission)



Scheda	Coordinator	# INAF Institutes	# INAF people
AGILE	C. Pittori	8	35
ET	<i>M. Branchesi</i>	13	55
Fermi Science	P. Caraveo	4	12
GAME	L. Piro	4	13
GRAWITA	E. Brocato	11	66
GRB@Mi	G. Ghirlanda	3	13
GRB@OAS	E. Pian	4	11
GuRu	S. Piranomonte	6	9
HERMES	F. Fiore	8	30
INTEGRAL	L. Natalucci	3	14
INTEGRAL HEASS	A. Malizia	3	14
LGWA	<i>J. Harms</i>	9	27
NuMerJet	R. Ciolfi	9	18
Progress	L. A. Antonelli	15	244
Swift	G. Tagliaferri	4	24

Multi-Messenger Astrophysics (GW) @ RSN4

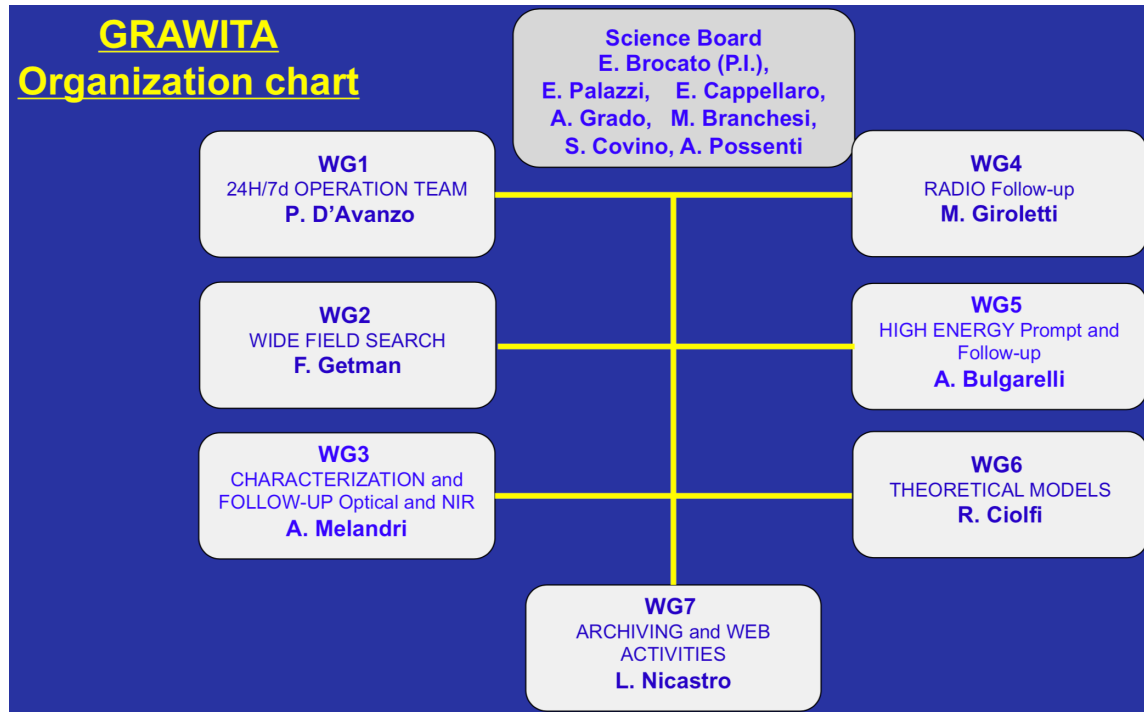
Discovery of the X-ray afterglow



Long-term monitoring of the off-axis GRB afterglow emission -> evidence for structured jet

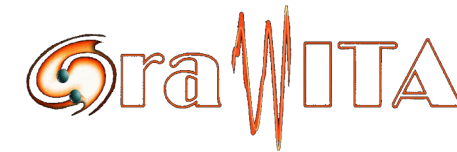
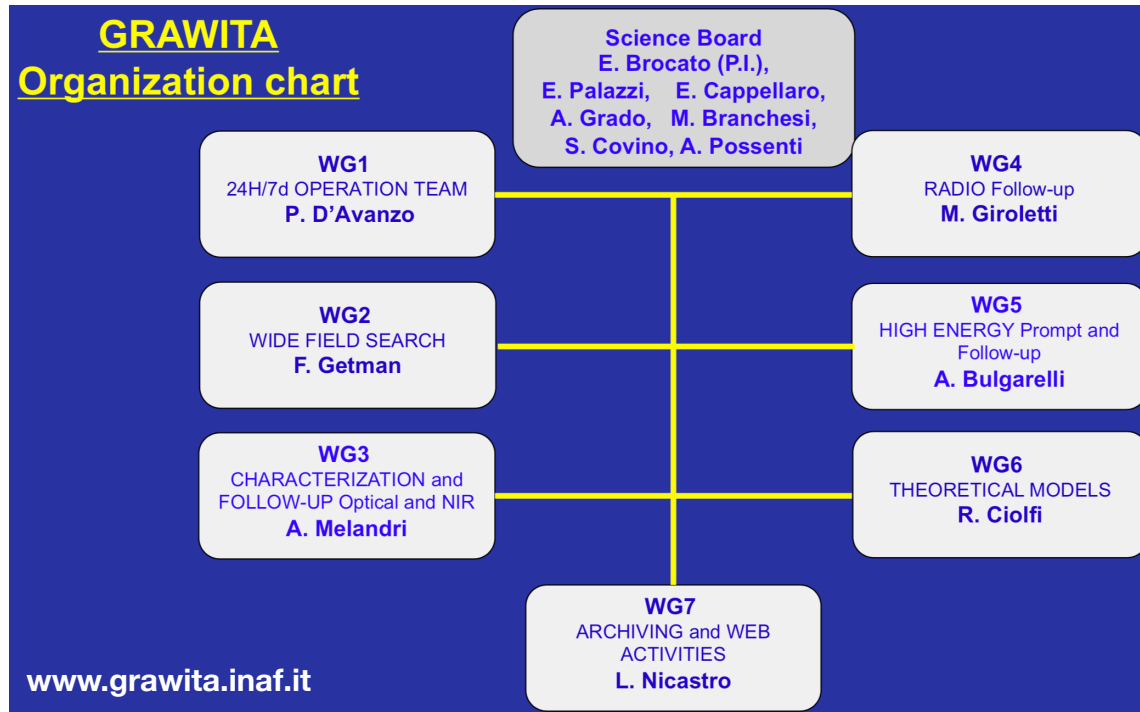
Scheda	Coordinator	# INAF Institutes	# INAF people
AGILE	C. Pittori	8	35
ET	<i>M. Branchesi</i>	13	55
Fermi Science	P. Caraveo	4	12
GAME	L. Piro	4	13
GRAWITA	E. Brocato	11	66
GRB@Mi	G. Ghirlanda	3	13
GRB@OAS	E. Pian	4	11
GuRu	S. Piranomonte	6	9
HERMES	F. Fiore	8	30
INTEGRAL	L. Natalucci	3	14
INTEGRAL HEASS	A. Malizia	3	14
LGWA	<i>J. Harms</i>	9	27
NuMerJet	R. Ciolfi	9	18
Progress	L. A. Antonelli	15	244
Swift	G. Tagliaferri	4	24

GRAvitational Wave Inaf TeAm



**~ 100 scientists
from 21 Institutes
(INAF + Universities)
Active since O1**

(Super-)GRAWITA & ENGRAVE



~ 100 scientists
from 21 Institutes
(INAF + Universities)
Active since O1

+

Coordination with AGILE, Fermi,
INTEGRAL & Swift INAF research
teams
(Super-GRAWITA, since O3)

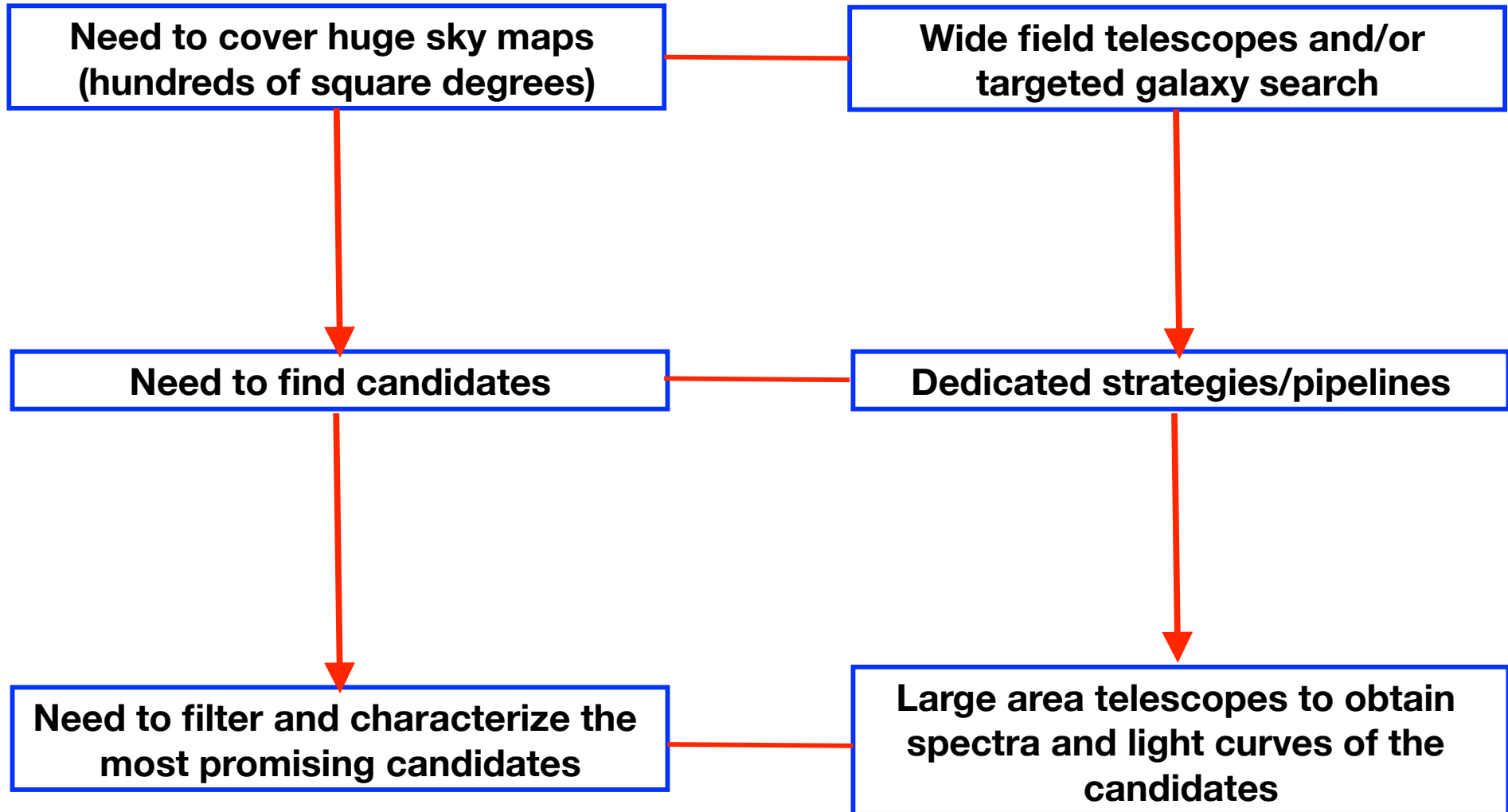


Governing Council: *M. Branchesi*, **E. Brocato**, **P. D'Avanzo**, J. Hjorth, P. Jonker, E. Pian, S. Smartt (Chair), J. Sollerman, D. Steeghs, N. Tanvir.
Executive Committee: A. Levan (Chair), M. Fraser, K. Maguire, *D. Malesani*, *O. S. Salafia*, *S. Vergani*.



A collaboration of ~ 200 ESO scientists (since O3)
Approved program during Oct 2018 – Mar 2020 fully covering O3. Time for EM counterparts **follow-up** on every useful **VLT** instrument + **ALMA** **HST** and **JWST**.

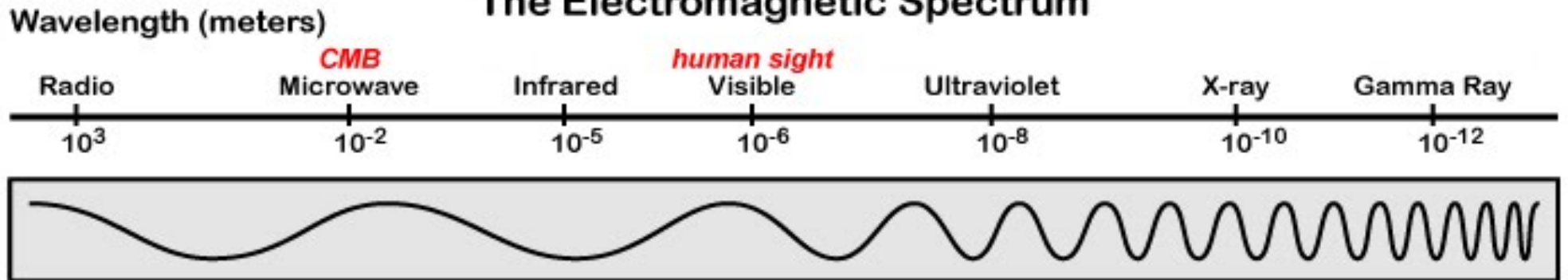
Follow-up strategy



Facilities in O4



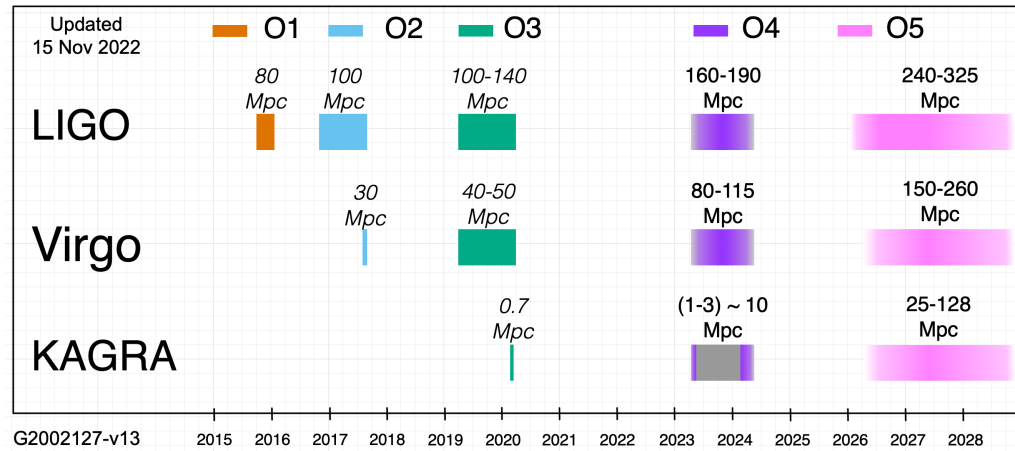
The Electromagnetic Spectrum



The Future

Beyond O4

Future Facilities



The Electromagnetic Spectrum

Wavelength (meters)

Radio

CMB
Microwave

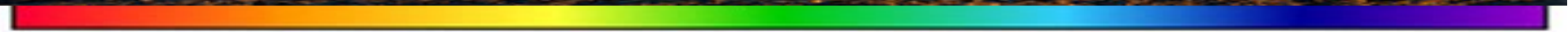
Infrared

human sight
Visible

Ultraviolet

X-ray

Gamma Ray

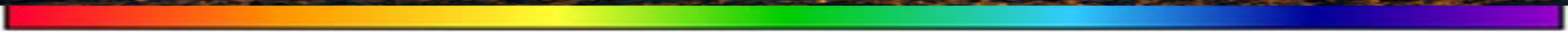
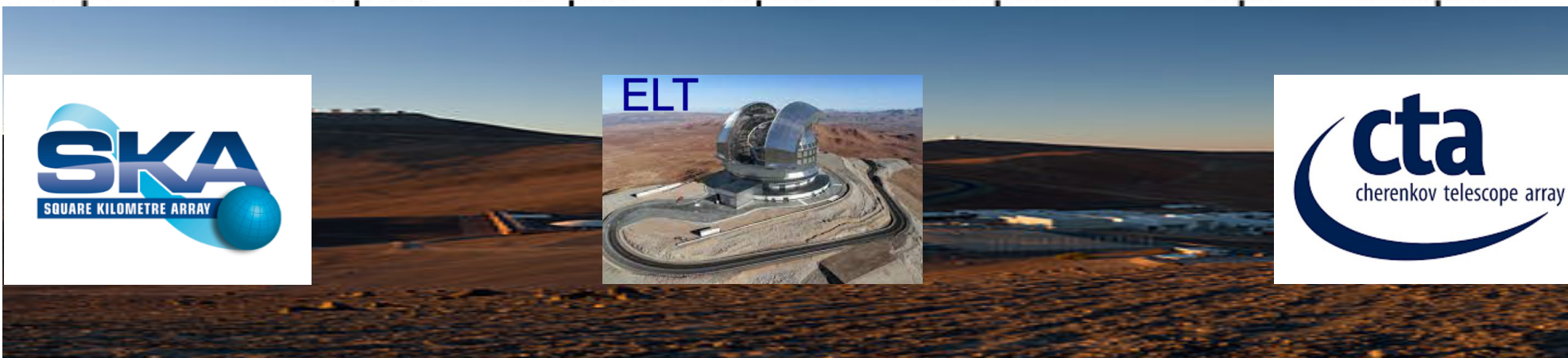


Future Facilities



Wavelength (meters)

Radio *CMB* Microwave Infrared *human sight* Visible Ultraviolet X-ray Gamma Ray



Final Thoughts

- A new era for astrophysics, great discovery space, opportunities for early career astronomers

- INAF at the forefront (worldwide) since the dawn of this era

- Leadership gained (also) thanks to the GRB (BeppoSAX & Swift) and SNe heritage

- Future can be (very) bright, but also hard (see O3)

- Importance of multi-wavelength and theoretical expertises -> importance of collaborations (also international)

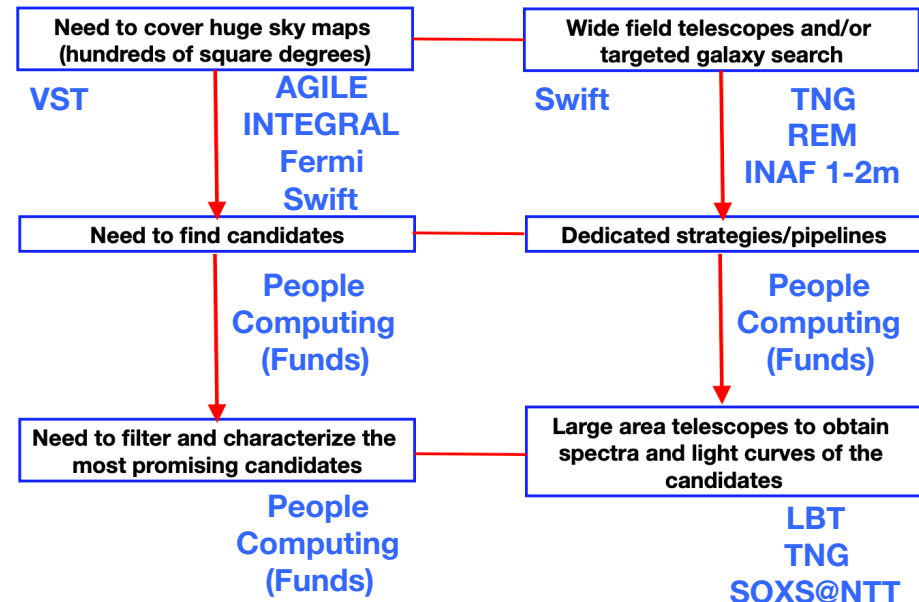
- Importance of flexible facilities, ToO, possibly dedicated

- ESO has (and will have) a very good ToO policy

- National facilities (at all scales) should be kept in operations, with a ToO policy (LBT and TNG have ToO, REM is robotic – great! - very good that VST will have -> to be improved!)

- Vital to keep as long as possible high-energy satellites

- Great SVOM will arrive soon, it would be fantastic to have THESEUS and Athena in the '30s



A new era just begun, great opportunities for breakthrough discoveries, INAF should keep sustaining at all levels (funds, facilities, recruitment, collaborations) this field, to keep leadership (worldwide) role.

GRAWITA will benefit from a Large Grant-> vital to reach the O4 horizon

